Biogeosciences Discuss., doi:10.5194/bg-2016-318, 2016
Manuscript under review for journal Biogeosciences
Published: 31 August 2016

Biogeosciences Discussions Open Access EGU

Hydrothermal activity lowers trophic diversity in Antarctic sedimented hydrothermal vents

James B. Bell[1,2]*, William D. K. Reid[3], David A. Pearce[4], Adrian G. Glover[2], Christopher J. Sweeting[5], Jason Newton[6], & Clare Woulds[1]

[1]School of Geography& Water@Leeds, University of Leeds, LS2 9JT, UK.
[2]Life Sciences Dept., Natural History Museum, Cromwell Rd, London SW7 5BD, UK
[3]Ridley Building, School of Biology, Newcastle University, NE1 7RU, UK
[4]Applied Sciences, Northumbria University, Newcastle, NE1 8ST, UK
[5]Ridley Building, School of Marine Science and Technology, Newcastle University, NE1 7RU, UK
[6]NERC Life Sciences Mass Spectrometry Facility, SUERC, East Kilbride G75 0QF, UK

* E-mail: gyjbb@leeds.ac.uk

Keywords: Stable Isotopes; Trophic Niche; Sedimented; Hydrothermal; Southern Ocean; Microbial; 16S; PLFA

Biogeosciences Discuss., doi:10.5194/bg-2016-318, 2016
Manuscript under review for journal Biogeosciences
Published: 31 August 2016

17 Abstract

18

19 Sedimented hydrothermal vents are those in which hydrothermal fluid vents through sediment
20 and are among the least studied deep-sea ecosystems. We present a combination of microbial
21 and biochemical data to assess trophodynamics between and within hydrothermally active and
22 off-vent areas of the Bransfield Strait (1050 – 1647m depth). Microbial composition, biomass
23 and fatty acid signatures varied widely between and within vent and non-vent sites and
24 provided evidence of diverse metabolic activity. Several species showed diverse feeding
25 strategies and occupied different trophic positions in vent and non-vent areas and stable
26 isotope values of consumers were generally not consistent with feeding structure morphology.
27 Niche area and the diversity of microbial fatty acids reflected trends in species diversity and
28 was lowest at the most hydrothermally active site. Faunal utilisation of chemosynthetic activity
29 was relatively limited but was detected at both vent and non-vent sites as evidenced by carbon
30 and sulphur isotopic signatures, suggesting that the hydrothermal activity can affect
31 trophodynamics over a much wider area than previously thought.

32

Biogeosciences Discuss., doi:10.5194/bg-2016-318, 2016
Manuscript under review for journal Biogeosciences
Published: 31 August 2016

33 Section 1. Introduction

34

35 As a result of subsurface mixing between hydrothermal fluid and ambient seawater within the
36 sediment, sedimented hydrothermal vents (SHVs) are more similar to non-hydrothermal deep-
37 sea habitats than they are to high temperature, hard substratum vents (Bemis et al. 2012,
38 Bernardino et al. 2012). This creates opportunities for non-specialist, soft-sediment fauna to
39 colonise areas of chemosynthetic organic matter production, potentially offering an important
40 metabolic resource in the nutrient-limited deep-sea (Levin et al. 2009, Dowell et al. 2016). To
41 take advantage of this resource, fauna must overcome the environmental stress associated
42 with high-temperature, acidic and toxic conditions at SHVs (Levin et al. 2013, Gollner et al.
43 2015). The combination of elevated toxicity and in-situ organic matter (OM) production results
44 in a different complement of ecological niches between vents and background conditions that
45 elicits compositional changes along a productivity-toxicity gradient (Bernardino et al. 2012,
46 Gollner et al. 2015, Bell et al. 2016). Hydrothermal sediments offer different relative
47 abundances of chemosynthetic and photosynthetic organic matter, depending upon supply of
48 surface-derived primary productivity, which may vary with depth and latitude, and levels of
49 hydrothermal activity (Tarasov et al. 2005). In shallow environments (<200 m depth), where
50 production of chemosynthetic and photosynthetic organic matter sources can co-occur,
51 consumption may still favour photosynthetic OM over chemosynthetic OM as this does not
52 require adaptions to environmental toxicity (Kharlamenko et al. 1995, Tarasov et al. 2005,
53 Sellanes et al. 2011). Limited information of trophodynamics at deep-sea SHVs indicate that
54 diet composition estimates vary widely between taxa, ranging between 0 – 87 % contribution
55 from chemosynthetic OM (Sweetman et al. 2013). Thus, understanding of the significance of
56 chemosynthetic activity in these settings is very limited.

57

Biogeosciences Discuss., doi:10.5194/bg-2016-318, 2016
Manuscript under review for journal Biogeosciences
Published: 31 August 2016

Sedimented hydrothermal vents host diverse microbial communities (Teske et al. 2002, Weber & Jørgensen 2002, Dhillon et al. 2003, Kallmeyer & Boetius 2004, Teske et al. 2014, Dowell et al. 2016). Microbial communities are a vital intermediate between hydrothermal fluid and metazoan consumers, and thus their composition and isotopic signatures are of direct relevance to metazoan food webs. The reduced chemical compounds and heat flux associated with hydrothermal activity provides thermodynamic benefits and constraints to microbial community assembly (Kallmeyer & Boetius 2004, Teske et al. 2014) but also accelerates the degradation of organic matter, giving rise to a wide variety of compounds, including hydrocarbons and organic acids (Martens 1990, Whiticar & Suess 1990, Dowell et al. 2016). Microbial aggregations are commonly visible on the sediment surface at SHVs (Levin et al. 2009, Aquilina et al. 2013, Sweetman et al. 2013, Dowell et al. 2016) but active communities are distributed throughout the underlying sediment layers, occupying a wide range of geochemical and thermal niches (reviewed by Teske et al. 2014). Sedimented vents may present several sources of organic matter to consumers (Bernardino et al. 2012, Sweetman et al. 2013) and the diverse microbial assemblages can support a variety of reaction pathways, including methane oxidation, sulphide oxidation, sulphate reduction and nitrogen fixation (Teske et al. 2002, Dekas et al. 2009, Frank et al. 2013, Jaeschke et al. 2014, Wu et al. 2014, Inskeep et al. 2015, McKay et al. 2015). Phospholipid fatty acid (PLFA) analysis can be used to describe recent microbial activity and $\delta^{13}C$ signatures (Kharlamenko et al. 1995, Boschker & Middelburg 2002, Colaço et al. 2007, Jaeschke et al. 2014). Although it can be difficult to ascribe a PLFA to a specific microbial group or process, high relative abundances of certain PLFAs can be strongly indicative of chemoautotrophy (Colaço et al. 2007).

Macrofaunal assemblages of the Bransfield SHVs (Bell et al. 2016) were strongly influenced by hydrothermal activity. Bacterial mats were widespread across Hook Ridge, where variable

Biogeosciences Discuss., doi:10.5194/bg-2016-318, 2016
Manuscript under review for journal Biogeosciences
Published: 31 August 2016

83 levels of hydrothermal activity were detected (Aquilina et al. 2013). Populations of siboglinid
84 polychaetes (*Sclerolinum contortum* and *Siboglinum* sp.), were found at Hook Ridge and non-
85 hydrothermally active sites (Sahling et al. 2005, Georgieva et al. 2015, Bell et al. 2016). These
86 species are known to harbour chemoautotrophic endosymbionts (Schmaljohann et al. 1990,
87 Gebruk et al. 2003, Thornhill et al. 2008, Eichinger et al. 2013, Rodrigues et al. 2013). Stable
88 isotope analysis (SIA) is a powerful tool to assess spatial and temporal patterns in faunal
89 behaviour and has been used to study trophodynamics and resource partitioning in other SHVs
90 (Southward et al. 2001, Levin et al. 2009, Soto 2009, Levin et al. 2012, Sweetman et al. 2013).
91 *Siboglinum* spp. in particular can use a range of resources, including methane or dissolved
92 organic matter (Southward et al. 1979, Schmaljohann et al. 1990, Thornhill et al. 2008,
93 Rodrigues et al. 2013), making SIA an ideal way in which to examine resource utilisation. We
94 also apply the concept of an isotopic niche (Layman et al. 2007) whereby species or community
95 trophic activity is inferred from the distribution of stable isotopic data in isotope space.
96
97 1.3. Hypotheses
98
99 We used a combination of microbial sequencing data and compound specific and bulk isotopic
100 data from sediment, microbial, macro- and megafaunal samples to investigate resource
101 utilisation, niche partitioning and trophic structure at vent and background sites in the
102 Bransfield Strait to test the following hypotheses: 1) Stable isotope signatures will reflect a-
103 priori functional designations defined by faunal morphology; 2) Fauna will have distinct niches
104 between vents and background areas; 3) Siboglinid species subsist upon chemosynthetically-
105 derived OM and 4) Chemosynthetic organic matter will be a significant food source at SHVs.

Biogeosciences Discuss., doi:10.5194/bg-2016-318, 2016
Manuscript under review for journal Biogeosciences
Published: 31 August 2016

106 Section 2. Materials and Methods

107

108 2.1. Sites and Sampling

109

110 Samples were collected; during RRS *James Cook* cruise JC55 in the austral summer of 2011
111 (Tyler et al. 2011), from three raised edifices along the basin axis (Hook Ridge, the Three
112 Sisters and The Axe, see Fig. 1 Bell et al. (2016) for map) and one off-axis site, in the Bransfield
113 Strait (1024 – 1311m depth). We visited two sites of variable hydrothermal activity; Hook
114 Ridge 1 and 2 (Aquilina et al. 2013) and three sites (Three Sisters, the Axe and an Off-Axis site)
115 where hydrothermal activity was not detected (Aquilina et al. 2013). Samples were collected
116 with a series of megacore deployments, using a Bowers & Connelly dampened megacorer
117 (1024 – 1311m depth) and a single Agassiz trawl at Hook Ridge (1647m depth). Except salps,
118 all microbial and faunal samples presented here were from megacore deployments. For a
119 detailed description of the megacore sampling programme and macrofaunal communities, see
120 Bell et al. (2016). Sampling consisted of 1 – 6 megacore deployments per site, with 2 – 5 tubes
121 pooled per deployment (Bell et al. 2016). Cores were sliced into 0 – 5cm and 5 – 10cm
122 partitions and macrofauna were retained on a 300 μm sieve. Residues were preserved in
123 either 80 % ethanol or 10 % buffered formalin initially and then stored in 80% ethanol after
124 sorting (Bell et al. 2016). Fauna were sorted to species/ morphospecies level (for annelid and
125 bivalve taxa); family level (for peracarids) and higher levels for less abundant phyla (e.g.
126 echiurans). Salps were collected using an Agassiz trawl and samples were immediately picked
127 and frozen at -80 ˚C and subsequently freeze-dried.

128

129 2.2. Microbiology Sequencing

130

Biogeosciences Discuss., doi:10.5194/bg-2016-318, 2016
Manuscript under review for journal Biogeosciences
Published: 31 August 2016

131 Samples of surface sediment (0 – 1 centimeters below seafloor (cmbsf)) were taken from
132 megacores the two Hook Ridge sites and the off-axis site and frozen (-80˚C). Sedimentary DNA
133 was extracted by Mr DNA (Shallowater, TX, USA) using an in-house standard 454 pipeline. The
134 resultant sequences were trimmed and sorted using default methods in Geneious (v.9.1.5 with
135 RDP v.2.8 and Krona v.2.0) and analysed in the Geneious '16 Biodiversity Tool'
136 (https://16s.geneious.com/16s/help.html) (Wang et al. 2007, Ondov et al. 2011, Biomatters
137 2014).
138
139 2.3. Phospholipid Fatty Acids
140
141 Samples of 3 – 3.5 g of freeze-dried sediment from Hook Ridge 1 & 2, the off-vent site and the
142 Three Sisters were analysed at the James Hutton Institute (Aberdeen, UK) following the
143 procedure detailed in Main et al. (2015), which we summarise below. Samples were from the
144 top 1 cm of sediment for all sites except Hook Ridge 2 where sediment was pooled from two
145 core slices (0 – 2 cm), due to sample mass limitations. Lipids were extracted following a
146 method adapted from Bligh (1959), using a single phase mixture of chloroform: methanol:
147 citrate buffer (1:2:0.8 v-v:v). Lipids were fractionated using 6 ml ISOLUTE SI SPE columns,
148 preconditioned with 5 ml chloroform. Freeze-dried material was taken up in 400 µL of
149 chloroform; vortex mixed twice and allowed to pass through the column. Columns were
150 washed in chloroform and acetone (eluates discarded) and finally 10 ml of methanol. Methanol
151 eluates were collected in vials, allowed to evaporate under a N_2 atmosphere and frozen at -20
152 ˚C.
153
154 PLFAs were derivitised with methanol and potassium hydroxide to produce fatty acid methyl
155 esters (FAMEs). Samples were taken up in 1 mL of 1:1 (v:v) mixture of methanol and toluene. 1

Biogeosciences Discuss., doi:10.5194/bg-2016-318, 2016
Manuscript under review for journal Biogeosciences
Published: 31 August 2016

156 mL of 0.2 M KOH (in methanol) was added with a known quantity of the C19 internal standard
157 (nonadecanoic acid), vortex mixed and incubated at 37 ˚C for 15 min. After cooling to room
158 temperature, 2 mL of isohexane:chloroform (4:1 v:v), 0.3 mL of 1 M acetic acid and 2 mL of
159 deionized water was added to each vial. The solution was mixed and centrifuged and the
160 organic phase transferred to a new vial and the remaining aqueous phase was mixed and
161 centrifuged again to further extract the organic phase, which was combined with the previous.
162 The organic phases were evaporated under a N_2 atmosphere and frozen at -20 ˚C.
163
164 Samples were taken up in isohexane to perform gas chromatography-combustion-isotope ratio
165 mass spectrometry (GC-C-IRMS). The quantity and $\delta^{13}C$ values of individual FAMEs were
166 determined using a GC Trace Ultra with combustion column attached via a GC Combustion III
167 to a Delta V Advantage isotope ratio mass spectrometer (Thermo Finnigan, Bremen). The
168 $\delta^{13}C_{VPDB}$ values (‰) of each FAME were calculated with respect to a reference gas of CO_2,
169 traceable to IAEA reference material NBS 19 TS-Limestone. Measurement of the Indiana
170 University reference material hexadecanoicacid methyl ester (certified $\delta^{13}C_{VPDB}$ 30.74
171 ± 0.01‰) gave a value of 30.91 ± 0.31‰ (mean ± sd, n=51). Combined areas of all mass peaks
172 (m/z 44, 45 and 46), following background correction, were collected for each FAME. These
173 areas, relative to the internal C19:0 standard, were used to quantify the 34 most abundant
174 FAMEs and related to the PLFAs from which they are derived (Thornton et al. 2011).
175
176 Bacterial biomass was calculated using transfer functions from the total mass of four PLFAs
177 (i14:0, i15:0, a15:0 and i16:0), estimated at 14 % of total bacterial PLFA, which in turn is
178 estimated at 5.6 % of total bacterial biomass (Boschker & Middelburg 2002).
179
180 2.4. Bulk Stable Isotopes

Biogeosciences Discuss., doi:10.5194/bg-2016-318, 2016
Manuscript under review for journal Biogeosciences
Published: 31 August 2016

181

182 All bulk isotopic analyses were completed at the East Kilbride Node of the Natural
183 Environment Research Council Life Sciences Mass Spectrometry Facility (EK). Specimens with
184 carbonate structures (e.g. bivalves) were physically decarbonated and all specimens were
185 rinsed and cleaned of attached sediment before drying. Specimens were dried for at least 24
186 hours at 50˚C and weighed (mg, correct to 3 d.p.) into tin capsules and stored in a desiccator
187 whilst awaiting SIA. Samples were analysed at EK by continuous flow isotope ratio mass
188 spectrometer using a Vario-Pyro Cube elemental analyser (Elementar), coupled with a Delta
189 Plus XP isotope ratio mass spectrometer (Thermo Electron). Each of the runs of CN and CNS
190 isotope analyses used laboratory standards (Gelatine and two amino acid-gelatine mixtures) as
191 well as the international standard USGS40 (glutamic acid). CNS measurements used the
192 internal standards (MSAG2: (Methanesulfonamide/ Gelatine and Methionine) and the
193 international silver sulphide standards IAEA-S1, S2 and S3. All sample runs included samples
194 of freeze-dried, powdered *Antimora rostrata* (ANR), an external reference material used in
195 other studies of chemosynthetic ecosystems (Reid et al. 2013, Bell et al. Accepted), used to
196 monitor variation between runs and instruments (supplementary file 1). Instrument precision
197 (S.D.) for each isotope measured from the reference material was 0.42, 0.33 and 0.54 for
198 carbon, nitrogen and sulphur respectively. The reference samples were generally consistent
199 except in one of the CNS runs, which showed unusual $\delta^{15}N$ measurements (S1), so faunal $\delta^{15}N$
200 measurements from this run were excluded as a precaution. Stable isotope ratios are all
201 reported in delta (δ) per mil (‰) notation, relative to international standards: V-PDB ($\delta^{13}C$);
202 Air ($\delta^{15}N$) and V-CDT ($\delta^{34}S$).

203

204 A combination of dual- ($\delta^{13}C$ & $\delta^{15}N$, 319 samples) and tri-isotope ($\delta^{13}C$, $\delta^{15}N$ & $\delta^{34}S$, 83
205 samples) techniques was used to describe bulk isotopic signatures of 43 species of macrofauna

Biogeosciences Discuss., doi:10.5194/bg-2016-318, 2016
Manuscript under review for journal Biogeosciences
Published: 31 August 2016

206 (35 from non-vent sites, 19 from vent sites and 11 from both), 3 megafaunal taxa and sources
207 of organic matter. Samples submitted for carbon and nitrogen (CN) analyses were pooled if
208 necessary to achieve an optimal mass of 0.7 mg (± 0.5 mg). Where possible, individual
209 specimens were kept separate in order to preserve variance structure within populations but
210 in some cases, low sample mass meant individuals had to be pooled (from individuals found in
211 replicate deployments). Optimal mass for Carbon-Nitrogen-Sulphur (CNS) measurements was
212 2.5 mg (± 0.5 mg) and, as with CN analyses, specimens were submitted as individual samples
213 or pooled where necessary. Samples of freeze-dried sediment from each site were also
214 submitted for CNS analyses (untreated for NS and acidified with 6M HCl for C) Acidification
215 was carried out by repeated washing with acid and de-ionised water.
216
217 Specimens were not acidified. A pilot study at EK, and subsequent results, confirmed that the
218 range in $\delta^{13}C$ measurements between acidified (0.1M and 1.0M HCl) was within the untreated
219 population range, in both polychaetes and peracarids and that acidification did not notably or
220 consistently reduce $\delta^{13}C$ standard deviation (Table 1). In the absence of a large or consistent
221 treatment effect, the low sample mass, (particularly for CNS samples) was dedicated to
222 increasing replication and preserving integrity of $\delta^{15}N$ & $\delta^{34}S$ measurements instead of
223 separating carbon and nitrogen/ sulphur samples (Connolly & Schlacher 2013).
224
225 Formalin and ethanol preservation effects can both influence the isotopic signature of a
226 sample. Taxa that had several samples of each preservation method from a single site (to
227 minimise intra-specific differences) were examined to determine the extent of isotopic shifts
228 associated with preservation effects. Carbon and nitrogen isotopic differences between ethanol
229 and formalin preserved samples ranged between 0.07 – 1.38 ‰ and 0.40 – 1.96 ‰
230 respectively. Differences across all samples were not significant (Paired t-test, $\delta^{13}C$: t = 2.10, df

Biogeosciences Discuss., doi:10.5194/bg-2016-318, 2016
Manuscript under review for journal Biogeosciences
Published: 31 August 2016

231 = 3, p = 0.126 and $\delta^{15}N$: t=1.14, df = 3, p = 0.337). Given the unpredictable response of isotopic
232 signatures to preservation effects in this case (which also cannot be extricated from within-
233 site, intraspecific variation) it was not possible to correct isotopic data. This contributed an
234 unavoidable, but generally quite small, source of error in these measurements.
235
236 2.5. Statistical Analyses
237
238 All analyses were completed in the R statistical environment (R Core Team 2013). Carbon and
239 nitrogen stable isotopic measurements were divided into those from vent or non-vent sites and
240 averaged by taxa and used to construct a Euclidean distance matrix (Valls et al. 2014). This
241 matrix was used to conduct a similarity profile routine (SIMPROF, 10 000 permutations, p =
242 0.05, Ward linkage) using the clustsig package (v1.0) (Clarke et al. 2008, Whitaker &
243 Christmann 2013) to test for significant structure within the matrix. The resulting cluster
244 assignations were compared to a-priori feeding groups (Bell et al. 2016) using a Spearman
245 Correlation Test (with 9 999 Monte Carlo resamplings) using the coin package (v1.0-24)
246 (Hothorn et al. 2015). Isotopic signatures of species sampled from both vent and non-vent sites
247 were also compared with a one-way ANOVA with Tukey's HSD pairwise comparisons
248 (following a Shapiro-Wilk normality test).
249
250 Mean faunal measurements of $\delta^{13}C$ & $\delta^{15}N$ were used to calculate Layman metrics for each site
251 (Layman et al. 2007), sample-size corrected standard elliptical area (SEAc) and Bayesian
252 posterior draws (SEA.B, mean of 10^5 draws ± 95% credibility interval) in the SIAR package
253 (v4.2) (Parnell et al. 2010, Jackson et al. 2011). Differences in SEA.B between sites were
254 compared in mixSIAR. The value of p given is the proportion of ellipses from group A that were
255 smaller in area than those from group B (e.g. if p = 0.02, then 2% of posterior draws from

Biogeosciences Discuss., doi:10.5194/bg-2016-318, 2016
Manuscript under review for journal Biogeosciences
Published: 31 August 2016

256 group A were smaller than the group B mean) and is considered to be a semi-quantitative

257 measure of difference in means (Jackson et al. 2011).

Biogeosciences Discuss., doi:10.5194/bg-2016-318, 2016
Manuscript under review for journal Biogeosciences
Published: 31 August 2016

258 Section 3. Results

259

260 3.1. Differences in microbial composition along a hydrothermal gradient

261

262 A total of 28,767, 35,490 and 47,870 sequences were obtained from the off-axis site, Hook
263 Ridge 1 and Hook Ridge 2 respectively. Bacteria comprised almost the entirety of each sample,
264 with Archaea being detected only in the Hook Ridge 2 sample (0.008 % of sequences). Hook
265 Ridge 1 was qualitatively more similar to the off-axis site than Hook Ridge 2. Both HR1 and
266 BOV were dominated by Proteobacteria (48 and 61 % of reads respectively; Fig. 1), whereas
267 Flavobacteriia dominated Hook Ridge 2 (43 %, 7 – 12 % elsewhere) with Proteobacteria
268 accounting for a smaller percentage of sequences (36 %; Fig. 1). By sequence abundance,
269 Flavobacteriia were the most clearly disparate group between Hook Ridge 2 and the other
270 sites. Flavobacteriia were comprised of 73 genera at Hook Ridge 2, 60 genera at BOV and 63
271 genera at HR1, of which 54 genera were shared between all sites. Hook Ridge 2 had 15 unique
272 flavobacteriial genera but these collectively accounted for just 0.85 % of reads, indicating that
273 compositional differences were mainly driven by relative abundance, rather than taxonomic
274 richness.

275

276 The most abundant genus from each site was *Arenicella* at BOV and HR1 (7.13 and 5.17 % of
277 reads respectively) and *Aestuariicola* at HR2 (6.89 % of reads). The four most abundant genera
278 at both BOV and HR1 were *Arenicella* (γ-proteobacteria), *Methylohalomonas* (γ-
279 proteobacteria), *Pasteuria* (Bacilli) & *Blastopirellula* (Planctomycetacia), though not in the
280 same order, and accounted for 17.22 and 15.97 % of reads respectively. The four most
281 abundant genera at HR2, accounting for 20.17 % of reads were *Aestuariicola*, *Lutimonas,*
282 *Maritimimonas* & *Winogradskyella* (all Flavobacteriia). The genera *Arenicella* and *Pasteuria*

Biogeosciences Discuss., doi:10.5194/bg-2016-318, 2016
Manuscript under review for journal Biogeosciences
Published: 31 August 2016

were the most relatively abundant across all sites (2.24 – 7.14 and 1.67 – 5.02 % of reads respectively).

3.2. Microbial stable isotopic signatures

A total of 37 sedimentary PLFAs were identified, in individual abundances ranging between 0 – 26.4 % of total PLFA (Table 2; Supplementary Fig 1). The most abundant PLFAs at each site were 16:0 (15.73 – 26.40 %), 16:1ω7c (11.50 – 20.00 %) and 18:1ω7 (4.80 – 16.85 %) (Table 2). PLFA profiles from each of the non-vent sites sampled (Off-axis and the Three Sisters, 33 and 34 PLFAs respectively) were quite similar (Table 2) and shared all but one compound (16:1ω11c, present only at the Three Sisters). Fewer PLFAs were enumerated from Hook Ridge 1 and 2 (31 and 23 respectively), including 3 PLFAs not observed at the non-vent sites (br17:0, 10-Me-17:0 & 10-Me-18:0), which accounted for 0.5 – 1.2 % of the total at these sites. Hook Ridge 2 had the lowest number of PLFAs and the lowest total PLFA biomass of any site, though this was due in part to the fact that this sample had to be pooled from the top 2 cm of sediment (top 1cm at other sites).

PLFA carbon isotopic signatures ranged -56 to -20 ‰ at non-vent sites and -42 to -8 ‰ at Hook Ridge (Table 2). Weighted average $\delta^{13}C$ values were quite similar between the non-vent sites and Hook Ridge 1 (-30.5 to -30.1 ‰), but were heavier at Hook Ridge 2 (-26.9 ‰; Table 2). Several of the PLFAs identified had a large range in $\delta^{13}C$ between samples (including 16:1ω11t $\delta^{13}C$ range = 17.15 ‰ or 19:1ω8 $\delta^{13}C$ range = 19.11 ‰), even between the non-vent sites (e.g. 18:2ω6, 9, $\Delta\delta^{13}C$ = 24.36; Table 2). Of the 37 PLFAs, 7 had a $\delta^{13}C$ range of > 10 ‰ but these were comparatively minor and individually accounted for 0 – 4.91 % of total abundance. Average $\delta^{13}C$ range was 6.31 ‰ and a further 11 PLFAs had a $\delta^{13}C$ range of > 5 ‰, including

Biogeosciences Discuss., doi:10.5194/bg-2016-318, 2016
Manuscript under review for journal Biogeosciences
Published: 31 August 2016

some of the more abundant PLFAs, accounting for 36.8 – 46.6 % at each site. PLFAs with small $\delta^{13}C$ ranges (< 5 ‰) accounted for 44.6 – 54.4 % of total abundance at each site.

3.3. Description of bulk isotopic signatures

Most faunal isotopic signatures were within a comparatively narrow range ($\delta^{13}C$: -30 to -20 ‰, $\delta^{15}N$: 5 to 15 ‰ and $\delta^{34}S$: 10 to 20 ‰) and more depleted isotopic signatures were usually attributable to siboglinid species (Fig. 2). *Siboglinum* sp. (found at all non-Hook Ridge sites) had mean $\delta^{13}C$ and $\delta^{15}N$ values of -41.43 ‰ and -8.86 ‰ respectively and *Sclerolinum contortum* (predominately from Hook Ridge 1 but found at both vent sites) had values of -20.52 ‰ and -5.27‰ respectively. Some non-endosymbiont bearing taxa (e.g. macrofaunal neotanaids from the off-axis site and megafaunal ophiuroids at Hook Ridge 2) also had notably depleted $\delta^{15}N$ signatures (means -3.56 and 2.57 ‰ respectively) (Fig. 2).

Isotopic signatures of sediment organic matter were similar between vents and non-vents for $\delta^{13}C$ and $\delta^{15}N$ but $\delta^{34}S$ was significantly greater at non-vent sites ($p < 0.05$, Table 3; Fig. 4). Variability was higher in vent sediments for all isotopic signatures. Faunal isotopic signatures for $\delta^{13}C$ and $\delta^{34}S$ ranged much more widely than sediment signatures and indicate that sediment organics were a mixture of two or more sources of organic matter. A few macrofaunal species had relatively heavy $\delta^{13}C$ signatures that exceeded -20 ‰ that suggested either a heavy source of carbon or contamination from marine carbonate (~0 ‰). Samples of pelagic salps from Hook Ridge had mean values for $\delta^{13}C$ of -27.43 ‰ (± 0.88) and $\delta^{34}S$ of 21.48 ‰ (± 0.74).

3.4. Comparing macrofaunal morphology and stable isotopic signatures

Biogeosciences Discuss., doi:10.5194/bg-2016-318, 2016
Manuscript under review for journal Biogeosciences
Published: 31 August 2016

333

334 Averaged species isotopic data were each assigned to one of four clusters (SIMPROF, p = 0.05;
335 Supplementary Figure 3). No significant correlation between a-priori (based on morphology)
336 and a-posteriori clusters (based on isotopic data) was detected (Spearman Correlation Test: Z
337 = -1.34; N = 43; p = 0.18) and consequently, we reject hypothesis one (trophic position
338 determined by morphology). Clusters were mainly discriminated based on $\delta^{15}N$ values and
339 peracarids were the only taxa to be represented in all of the clusters, indicating high trophic
340 diversity.

341

342 Several taxa found at both vent and non-vent sites (Hook Ridge or the non-vent sites, Off-axis,
343 The Three Sisters and The Axe) were assigned to different clusters between sites. A total of
344 eleven taxa were sampled from both vent and non-vent regions, of which four were assigned to
345 different clusters at vent and non-vent sites. Neotanaids (Peracarida: Tanaidacea) had the
346 greatest Euclidean distance between vent/ non-vent samples (11.36), demonstrating clear
347 differences in dietary composition (Fig. 3) but all other species were separated by much
348 smaller distances between regions, ranging 0.24 to 2.69. Raw $\delta^{13}C$ and $\delta^{15}N$ values were also
349 compared between vent and non-vent samples for each species (one-way ANOVA with Tukey
350 HSD pairwise comparisons). Analysis of the raw data indicated that $\delta^{13}C$ signatures were
351 different for neotanaids only and $\delta^{15}N$ were different for neotanaids and an oligochaete species
352 (*Limnodriloides* sp.) (ANOVA, $p < 0.01$, Fig. 3).

353

354 3.5. Community-level trophic metrics

355

356 All site niches overlapped (mean = 50 %, range = 30 – 82 %) and the positions of ellipse
357 centroids were broadly similar for all sites (Table 4; Fig 5). Hook Ridge 1 & 2 ellipse areas were

Biogeosciences Discuss., doi:10.5194/bg-2016-318, 2016
Manuscript under review for journal Biogeosciences
Published: 31 August 2016

358 similar but significantly smaller than non-vent ellipses (SEA.B, n = 10^5, p = < 0.05). There were
359 no significant differences in ellipse area between any non-vent sites. Ranges in carbon sources
360 (dCr) were higher for non-vent sites (Table 4) indicating a greater trophic diversity in
361 background conditions. Nitrogen range (dNr, Table 4) was similar between vents and non-
362 vents suggesting a similar number of trophic levels within each assemblage. All site ellipses
363 had broadly similar eccentricity, ranging 0.85 – 0.97 (Table 4) but theta differed between vent
364 and non-vent sites (-1.43 to 1.55 at Hook Ridge, 0.67 to 0.86 at non-vent sites). Range in
365 nitrogen sources was more influential at vent sites with *Sclerolinum contortum*, which had low
366 $\delta^{15}N$ signatures, had similar to $\delta^{13}C$ to non-endosymbiont bearing taxa. The strongly depleted
367 $\delta^{13}C$ measurements of *Siboglinum* sp. meant that ellipse theta was skewed more towards
368 horizontal (closer to zero) for non-vent sites.
369

Biogeosciences Discuss., doi:10.5194/bg-2016-318, 2016
Manuscript under review for journal Biogeosciences
Published: 31 August 2016

370 Section 4. Discussion

371

372 4.1. Microbial signatures of hydrothermal activity

373

374 PLFA profiles between the off-axis site and the Three Sisters indicated similar bacterial
375 biomass at each of these non-vent sites but that bacterial biomass varied much more widely at
376 Hook Ridge (Table 2). The Hook Ridge 2 sample is not directly comparable to the others as it
377 was sampled from sediment 0 – 2 cmbsf (owing to sample mass availability), though the
378 relatively low organic carbon content, hydrogen sulphide flux and taxonomic diversity at this
379 site may support suggestion of a lower overall bacterial biomass (Aquilina et al. 2013, Bell et al.
380 2016). The very high bacterial biomass at Hook Ridge 1 suggests a potentially very active
381 bacterial community but $\delta^{13}C$ was qualitatively similar to non-vent sites, implying that
382 chemosynthetic activity was comparatively limited, or that the isotopic signatures of the
383 carbon source (e.g. DIC) and the fractionation associated with FA synthesis resulted in similar
384 $\delta^{13}C$ signatures. Hook Ridge 1 PLFA composition was intermediate between non-vent sites and
385 Hook Ridge 1 (Supplementary Fig. 2) but sequence composition was quite similar between
386 Hook Ridge 1 and the off-axis site (Fig. 1). A small number of the more abundant PLFAs had
387 notable for differences in relative abundance between vent/ non-vent sites (Table 2). For
388 example, 16:1ω7, which has been linked to sulphur cycling pathways (Colaço et al. 2007)
389 comprised 13.95 – 15.19 % of abundance at non-vent sites and 20.00 – 23.50 % at vent sites.
390 However 18:1ω7, also a suggested PLFA linked to thio-oxidation occurred in lower abundance
391 at vent sites (4.80 – 11.12 %) than non-vent sites (15.91 – 16.85 %). This further suggests that
392 chemosynthetic activity was relatively limited since, although there were differences in
393 microbial signatures of chemosynthetic activity, these were not necessarily consistent between
394 different PLFAs.

Biogeosciences Discuss., doi:10.5194/bg-2016-318, 2016
Manuscript under review for journal Biogeosciences
Published: 31 August 2016

395

396 Several PLFAs had isotopic signatures that varied widely between sites, demonstrating
397 differences in fractionation and/ or source isotopic signatures. The heaviest PLFA $\delta^{13}C$
398 signatures were associated with Hook Ridge sites and were quite variable (e.g. 16:1ω11t at
399 HR2, $\delta^{13}C$ = -8.65, ~-24 to -25 ‰ elsewhere). This provides strong evidence of isotopic
400 differences in the sources or metabolic pathways used to synthesise these FAs. Heavier carbon
401 isotopic signatures (> -15 ‰) are generally associated with rTCA cycle carbon fixation (Hugler
402 & Sievert 2011, Reid et al. 2013), suggesting that this pathway was active at this site, albeit at
403 probably quite low rates. Conversely, many of the lightest $\delta^{13}C$ signatures (e.g. 19:1ω8, -56.57
404 ‰, off-axis site) were associated with the non-vent sites. *Siboglinum* isotopic data
405 demonstrates that methanotrophy was probably occurring at these sites, and these depleted
406 PLFA isotopic signatures provides further evidence of methanotrophy, in free-living
407 sedimentary bacteria. Chemotrophic bacterial sequences (e.g. *Blastopirellula* (Schlesner 2015)
408 or *Rhodopirellula* (Bondoso et al. 2014)) were found at all sites in relatively high abundance,
409 suggesting widespread and active chemosynthesis, though the lack of a particularly dominant
410 bacterial group associated with chemosynthetic activity suggested that the supply of
411 chemosynthetic OM was likely relatively limited. Some PLFAs also had marked differences in
412 $\delta^{13}C$ signatures, even where there was strong compositional similarity between sites (i.e. the
413 non hook ridge sites). This suggested that either there were differences in the isotopic values
414 of inorganic or organic matter sources or that different bacterial metabolic pathways were
415 active. Between the non-vent sites, these PLFAs included PUFAs such as 18:2ω6, 9 ($\Delta\delta^{13}C$ 24.36
416 ‰) and 19:1ω8 ($\Delta\delta^{13}C$ 19.11 ‰). Differences in PLFA $\delta^{13}C$ between Hook Ridge sites also
417 ranged widely, with the largest differences being associated with PLFAs such as 16:1ω11t
418 ($\Delta\delta^{13}C$ 17.15 ‰) and 10-Me-16:0 ($\Delta\delta^{13}C$ 11.02 ‰). A number of these PLFAs have been linked
419 to chemoautotrophy, such as 10-Me-16:0 (*Desulfobacter* or *Desulfocurvus,* Sulphate reducers)

Biogeosciences Discuss., doi:10.5194/bg-2016-318, 2016
Manuscript under review for journal Biogeosciences
Published: 31 August 2016

(Colaço et al. 2007, Klouche et al. 2009, Boschker et al. 2014) and their presence is consistent with the hydrothermal signature of the sediment microbial community. However, it should be stressed that all PLFAs with larger $\delta^{13}C$ ranges were comparatively rare and never individually exceeded 5% of total abundance. This provides further evidence of limited chemosynthetic activity at all sites and is consistent with the presence of bacteria associated with methane and sulphur cycling. Microbial signatures, whilst supporting the suggestion of chemosynthetic activity, are not indicative of chemosynthetic OM being the dominant source of organic matter to food webs at any site (hypothesis four).

4.2. Siboglinids

Both species of siboglinid (*Sclerolinum contortum* from Hook Ridge and *Siboglinum* sp. from the non-vent sites) were clearly subsisting upon chemosynthetically derived organic matter, as evidenced by their morphology and strongly depleted isotopic signatures (Fig. 2). Nitrogen values for both species ($\delta^{15}N$ *Sclerolinum* = -5.27 ‰ ± 1.03, *Siboglinum* = -8.85 ‰ ± 0.79) clearly indicated reliance upon locally fixed N_2 (Rau 1981, Dekas et al. 2009, Dekas et al. 2014, Wu et al. 2014) rather than utilisation of sediment nitrogen ($\delta^{15}N$ = 5.73 ‰ ± 0.71). This supports hypothesis three, confirming that the siboglinid species were subsisting upon chemosynthetic OM, most likely supplied by their endosymbionts. Diazotrophy, facilitated by sulphate-reducing bacteria may be accelerated in sediments enriched with methane and has been possibly observed at other SHVs (Weber & Jørgensen 2002, Dhillon et al. 2003, Frank et al. 2013), consistent with the depleted $\delta^{15}N$ and $\delta^{34}S$ signatures of both siboglinid species (Fig. 2; 4).

Biogeosciences Discuss., doi:10.5194/bg-2016-318, 2016
Manuscript under review for journal Biogeosciences
Published: 31 August 2016

444 Carbon isotopic signatures in chemosynthetic primary production depend upon the mode of
445 fixation and the initial $\delta^{13}C$ of available DIC. *Sclerolinum contortum* $\delta^{13}C$ (-20.52 ‰ ± 0.99) was
446 depleted in $\delta^{13}C$ relative to Southern Ocean DIC by around10 ‰ (Henley et al. 2012, Young et
447 al. 2013), giving it a signal within the fractionation range of the reverse tricarboxylic acid
448 cycle (Yorisue et al. 2012). Regional measurements of surface ocean DIC $\delta^{13}C$ have an average
449 isotopic signature of -10.37 ‰ (Henley et al. 2012, Young et al. 2013) but the concentration
450 and isotopic composition of DIC can undergo considerable alteration at sedimented vents
451 (Walker et al. 2008) and consequently, may exhibit substantial variation in $\delta^{13}C$. Therefore,
452 without measurements of $\delta^{13}C$ in pore fluid DIC, it was not possible to determine which
453 fixation pathway(s) were being used by *S. contortum* endosymbionts.
454
455 Sulphur isotopic signatures in *S. contortum* were very depleted, and quite variable ($\delta^{34}S$ -26.65
456 ‰ ± 3.47). *Sclerolinum* endosymbionts may have been utilising sulphide re-dissolved from
457 hydrothermal precipitates present at Hook Ridge that ranged between -28.1 to +5.1 (Petersen
458 et al. 2004), consistent with the relatively high $\delta^{34}S$ variability in *S. contortum*. Alternatively,
459 sulphide supplied as a result of microbial sulphate reduction (Canfield 2001) may have been
460 the primary source of organic sulphur, similar to that of solemyid bivalves from reducing
461 sediments near a sewage pipe outfall (mean $\delta^{34}S$ ranged -30 to -20 ‰ (Vetter & Fry 1998)).
462 Sulphate reduction can also be associated with anaerobic oxidation of methane (Whiticar &
463 Suess 1990, Canfield 2001, Yoshinaga et al. 2014, Cerqueira et al. 2015, Dowell et al. 2016),
464 suggesting that methanotrophic pathways could also have been important at Hook Ridge. (e.g.
465 abundance of *Methylohalomonas*, 2.08 – 4.28 % of sequences at all sites). Although
466 endosymbiont composition data are not available for the Southern Ocean population,
467 *Sclerolinum contortum* is also known from hydrocarbon seeps in the Gulf of Mexico (Eichinger
468 et al. 2013, Eichinger et al. 2014, Georgieva et al. 2015) and the Håkon Mosby mud volcano in

Biogeosciences Discuss., doi:10.5194/bg-2016-318, 2016
Manuscript under review for journal Biogeosciences
Published: 31 August 2016

469 the Arctic ocean, where *S. contortum* $\delta^{13}C$ ranged between -48.3 to -34.9 ‰ (Gebruk et al.
470 2003) demonstrating that this species is capable of occupying several reducing environments
471 and using a range of chemosynthetic fixation pathways, including sulphide oxidation and
472 methanotrophy (Eichinger et al. 2014, Georgieva et al. 2015).
473
474 *Siboglinum* sp. $\delta^{13}C$ values (mean -41.43, range -45.73 to -38.10 ‰, n = 8) corresponded very
475 closely to published values of thermogenic methane (-43 to -38 ‰) from the Bransfield Strait
476 (Whiticar & Suess 1990). Biogenic methane typically has much lower $\delta^{13}C$ values (Whiticar
477 1999), indicating a hydrothermal source of methane in the Bransfield Strait. Sulphur isotopic
478 signatures were also strongly depleted in *Siboglinum* sp. ($\delta^{34}S$ -22.85 ‰, one sample from 15
479 pooled individuals from the off-axis site), the most depleted measurement of $\delta^{34}S$ reported for
480 this genus (Schmaljohann & Flügel 1987, Rodrigues et al. 2013). The depleted $\delta^{13}C$, $\delta^{15}N$ and
481 $\delta^{34}S$ signatures of *Siboglinum* sp. suggest that its symbionts most likely included
482 methanotrophs, sulphate reducers and diazotrophs (Boetius et al. 2000, Canfield 2001, Dekas
483 et al. 2009). Methanotrophy in *Siboglinum* spp. has been previously documented at seeps in the
484 NE Pacific (Bernardino & Smith 2010) and Norwegian margin ($\delta^{13}C$ = -78.3 to -62.2 ‰)
485 (Schmaljohann et al. 1990) and in Atlantic mud volcanoes ($\delta^{13}C$ range -49.8 to -33.0 ‰)
486 (Rodrigues et al. 2013). Sulphur isotopic signatures in *Siboglinum* spp. from Atlantic mud
487 volcanoes ranged between -16.8 to 6.5 ‰ (Rodrigues et al. 2013) with the lowest value still
488 being 6 ‰ greater than that of Bransfield strait specimens. Rodrigues et al. (2013) also
489 reported a greater range in $\delta^{15}N$ than observed in the Bransfield siboglinids ($\delta^{15}N$ -1.3 to 12.2
490 ‰ and -10.16 to -7.63 ‰ respectively). This suggests that, in comparison to *Siboglinum* spp. in
491 Atlantic Mud volcanoes, which seemed to be using a mixture of organic matter sources
492 (Rodrigues et al. 2013), the Bransfield specimens relied much more heavily upon a single OM
493 source, suggesting considerable trophic plasticity in this genus worldwide.

Biogeosciences Discuss., doi:10.5194/bg-2016-318, 2016
Manuscript under review for journal Biogeosciences
Published: 31 August 2016

494

495 Off-vent methanotrophy, using thermogenic methane, (Whiticar & Suess 1990) potentially
496 illustrates an indirect dependence upon hydrothermalism. Sediment methane production is
497 thought to be accelerated by the heat flux associated with mixing of hydrothermal fluid in
498 sediment (Whiticar & Suess 1990) and thus, sediment and *Siboglinum* isotopic data suggest
499 that the footprint of hydrothermal influence may be much larger than previously recognised,
500 giving rise to transitional environments (Levin et al. 2016, Bell et al. Accepted). Clear
501 contribution of methane-derived carbon to consumer diets was limited predominately to
502 neotanaids, consistent with the relatively small population sizes (64 – 159 ind. m^2) of
503 *Siboglinum* sp. observed in the Bransfield Strait (Bell et al. 2016).

504

505 4.3. Organic Matter Sources

506

507 Pelagic salps, collected from an Agassiz trawl at Hook Ridge (1647m), were presumed to most
508 closely represent a diet of entirely surface-derived material and were more depleted in $\delta^{13}C$
509 and more enriched in ^{34}S than sediments (Table 3). Salp samples had a mean $\delta^{13}C$ of -27.43 ‰,
510 which was also lighter than the majority of macrofauna, both at Hook Ridge and the non-vent
511 sites (Fig. 2) and similar to other suspension feeding fauna in the Bransfield Strait (Elias-Piera
512 et al. 2013). This suggests that fauna with more depleted $\delta^{34}S$/ more enriched $\delta^{13}C$ values are
513 likely to have derived at least a small amount of their diet from chemosynthetic sources, both
514 at vents and background regions. Carbon and sulphur isotopic measurements indicated mixed
515 sources for most consumers between chemosynthetic OM and surface-derived photosynthetic
516 OM. Non-vent sediments were more enriched in ^{34}S than vent sediments, an offset that
517 probably resulted from greater availability of lighter sulphur sources such as sulphide
518 oxidation at Hook Ridge.

Biogeosciences Discuss., doi:10.5194/bg-2016-318, 2016
Manuscript under review for journal Biogeosciences
Published: 31 August 2016

519

520 Samples of bacterial mat could not be collected during JC55 (Tyler et al. 2011) and without
521 these endmember measurements, it was not possible to quantitatively model resource
522 partitioning in the Bransfield Strait using isotope mixing models (Phillips et al. 2014). Bacterial
523 mats from high-temperature vents in the Southern Ocean had $\delta^{34}S$ values of 0.8 ‰ (Reid et al.
524 2013) and at sedimented areas of the Loki's Castle hydrothermal vents in the Arctic Ocean has
525 $\delta^{34}S$ values of -4.9 ‰ (Bulk sediment; Jaeschke et al. 2014). Therefore it is probable that
526 depleted faunal $\delta^{34}S$ values represent a contribution of chemosynthetic OM (from either
527 siboglinid tissue or free-living bacteria). Inorganic sulphur can also be a source to consumers
528 when sulphide deposits are utilised by free living bacteria ($\delta^{34}S$ ranged -7.3 to 5.4 ‰ (Erickson
529 et al. 2009)) and sulphide crusts have been found at Hook Ridge ($\delta^{34}S$ -28.1 to 5.1 ‰ (Petersen
530 et al. 2004)). There were several species (e.g. Tubificid oligochaetes) that had moderately
531 depleted $\delta^{34}S$ signatures. *Limnodriloides* sp. had distinct $\delta^{34}S$ signatures between sites (7.56 ‰
532 at vents, -1.21 ‰ at non-vents, Fig. 4) further supporting the hypothesis of different trophic
533 positions between vent/ non-vent regions (hypothesis two). This provides evidence of coupled
534 AOM/sulphate reduction but overall, the contribution of $\delta^{34}S$-depleted bacterial production did
535 not seem widespread (further rejecting hypothesis four).

536

537 Without samples of all OM sources we cannot quantitatively assert that faunal utilisation of
538 chemosynthetic OM was low in the Bransfield Strait. Although isotopic data were consistent
539 with several OM sources, it seemed unlikely that chemosynthetic OM was a dominant source of
540 OM to the vast majority of taxa. The apparently limited consumption of chemosynthetic OM
541 suggested that either it was not widely available (e.g. patchy or low density of endosymbiont-
542 bearing fauna (Bell et al. 2016)), or that the ecological stress associated with feeding in areas of

Biogeosciences Discuss., doi:10.5194/bg-2016-318, 2016
Manuscript under review for journal Biogeosciences
Published: 31 August 2016

543 in situ production was a significant deterrent to many species (Bernardino et al. 2012, Levin et
544 al. 2013).
545
546 4.4. A-priori vs. a-posteriori trophic groups
547
548 Morphology did not prove to be an accurate predictor of trophic associations, suggesting that
549 faunal behaviour is potentially more important in determining dietary composition than
550 morphology (e.g. having/ lacking jaws). Peracarid species that possessed structures adapted to
551 a motile, carnivorous lifestyle were assigned to a carnivore/ scavenger guild (Bell et al. 2016)
552 but were distributed throughout the food web both at vents and background regions,
553 indicating more diverse feeding strategies than expected. Taxa presumed to be deposit feeders
554 (largely annelids) also had a surprisingly large range of $\delta^{15}N$ values. This may reflect the
555 consumption of detritus from both 'fresh' and more recycled sources as observed in other non-
556 vent sedimented deep-sea habitats (Iken et al. 2001, Reid et al. 2012) or reflect variability in
557 trophic discrimination related to diet quality (Adams & Sterner 2000). The result is high $\delta^{15}N$
558 values in taxa without predatory morphology (e.g. oligochaetes. Tubificid oligochaetes had
559 higher $\delta^{15}N$ values at the vent sites, suggesting that they fed upon more recycled organic
560 matter, possibly owing to greater microbial activity at vent sites. Bacterial biomass was very
561 variable at the vent sites (86 – 535 mg C m^{-2}, compared with 136 – 197 at non-vent sites; Table
562 2) and so it is possible that at Hook Ridge 1 bacterial assemblages could have had a greater
563 influence upon $\delta^{15}N$ of organic matter.
564
565 Neotanaids from the off-axis site had the most depleted $\delta^{13}C$ and $\delta^{15}N$ values of any non-
566 siboglinid taxon (Fig. 3), suggesting a significant contribution of methane-derived carbon. The
567 clustering of the neotanaids together with endosymbiont-bearing taxa is far more likely to be

Biogeosciences Discuss., doi:10.5194/bg-2016-318, 2016
Manuscript under review for journal Biogeosciences
Published: 31 August 2016

568 an artifact of the cluster linkage method, introduced by consumption of low $\delta^{13}C$
569 methanotrophic sources (e.g. *Siboglinum* tissue), rather than suggesting symbionts in these
570 fauna (Larsen 2006, Levin et al. 2009).
571
572 Several taxa (e.g. neotanaids from the off-axis site and ophiuroids at Hook Ridge) had low $\delta^{15}N$
573 values relative to sediment OM, suggesting preferential consumption of chemosynthetic OM
574 (Rau 1981, Dekas et al. 2014). In these taxa, it is likely that the widespread, but patchy
575 bacterial mats or *Sclerolinum* populations at Hook Ridge (Aquilina et al. 2013) was an
576 important source of organic matter to fauna with low $\delta^{15}N$ values (e.g. ophiuroids). Fauna from
577 the non-vent sites with low $\delta^{15}N$ were likely subsisting in part upon siboglinid tissue
578 (*Siboglinum* sp.). There were no video transects over the off-axis site but footage of the Three
579 Sisters (similar in macrofaunal composition (Bell et al. 2016)) did not reveal bacterial mats
580 (Aquilina et al. 2013), hence it is unlikely that these were a significant resource at non-vent
581 sites.
582
583 It is clear that some fauna can exhibit a degree of trophic plasticity, depending upon habitat
584 (supporting hypothesis two). This is consistent with other SHVs where several taxa (e.g.
585 *Prionospio* sp. – Polychaeta: Spionidae) had different isotopic signatures, depending upon their
586 environment (Levin et al. 2009), demonstrating differential patterns in resource utilisation.
587 Alternatively, there could have been different $\delta^{15}N$ baselines between sites, though if these
588 differences were significant, we argue that it likely that more species would have had
589 significant differences in tissue $\delta^{15}N$.
590
591 4.5. Impact of hydrothermal activity on community trophodynamics
592

Biogeosciences Discuss., doi:10.5194/bg-2016-318, 2016
Manuscript under review for journal Biogeosciences
Published: 31 August 2016

593 Standard ellipse area was lower at Hook Ridge than at non-vent sites (Table 4), analogous to
594 trends in macrofaunal diversity and abundance (Bell et al. 2016). This demonstrates that at
595 community level, SEA.B is associated with other macrofaunal assemblage characteristics. This
596 concurrent decline in niche area and alpha diversity is consistent with the concept that species
597 have finely partitioned niches and greater total niche area permits higher biodiversity (McClain
598 & Schlacher 2015). Productivity-diversity relationships, whereby higher productivity sustains
599 higher diversity, have also been suggested in the deep-sea (McClain & Schlacher 2015, Woolley
600 et al. 2016) but in the absence of measurements of in situ organic matter fixation rates at Hook
601 Ridge, it is unclear whether such relationships exist in the Bransfield Strait. Sediment organic
602 carbon content was similar between Hook ridge 1 and non-vent sites (1.35 – 1.40 %) but was
603 slightly lower at Hook Ridge 2 (0.97 %) (Bell et al. 2016), which is not consistent with variation
604 in niche area. The decline in alpha diversity and niche area is consistent with the influence of
605 disturbance gradients created by hydrothermalism that result in an impoverished community
606 (McClain & Schlacher 2015, Bell et al. 2016). We suggest that, in the Bransfield Strait, the
607 environmental toxicity at SHVs causes a concomitant decline in both trophic and species
608 diversity (Bell et al. 2016), in spite of the potential for increased localised production.
609
610 Community-based trophic metrics (Layman et al. 2007) indicated that, although measures of
611 dispersion within sites were relatively similar between vents and background areas (Table 4),
612 trophic diversity, particularly in terms of range of carbon sources (dCr) and total hull area (TA)
613 was higher at background sites. It was expected that trophic diversity would be greater at
614 Hook Ridge but the greater dCr at non-vent sites (owing to the methanotrophic source) meant
615 that the size isotopic niches at these sites was greater. Range in Nitrogen values (dNr) was also
616 greater at non-vents, driven by the more heavily depleted $\delta^{15}N$ values of *Siboglinum* sp.
617 Differences in eccentricity are more influenced by the spread of all isotopes used to construct

Biogeosciences Discuss., doi:10.5194/bg-2016-318, 2016
Manuscript under review for journal Biogeosciences
Published: 31 August 2016

618 the niche space (where E = 0 corresponds to an equal influence of both carbon and nitrogen)
619 whereas theta (the angle of the long axis) determines which, if any, isotope is most influential
620 in determining ellipse characteristics (Reid et al. 2016). For the non-vent sites, the dominant
621 isotope was carbon, owing to the relatively light $\delta^{13}C$ of methanotrophic source utilised by
622 *Siboglinum*. Some sites, particularly the Axe, had several fauna with heavy $\delta^{13}C$ values (Fig. 5),
623 which could be explained by either contamination from marine carbonate (~0 ‰), as
624 specimens were not acidified, or a diet that included a heavier source of carbon, such as sea ice
625 algae (Henley et al. 2012).
626

Biogeosciences Discuss., doi:10.5194/bg-2016-318, 2016
Manuscript under review for journal Biogeosciences
Published: 31 August 2016

627 Section 5. Conclusions

628

629 In this study, we demonstrate the influence of sediment-hosted hydrothermal venting upon
630 trophodynamics and microbial populations. Low activity vent microbiota were more similar to
631 the non-vent site than to high activity populations, illustrating the effect of ecological gradients
632 upon deep-sea microbial diversity. Despite widespread bacterial mats, and populations of vent-
633 endemic macrofauna, utilisation of chemosynthetic OM amongst non-specialist macro- and
634 megafauna seemed relatively low, with a concomitant decline in trophic diversity with
635 increasing hydrothermal activity. Morphology was also not indicative of trophic relationships,
636 demonstrating the effects of differential resource availability and behaviour. We suggest that,
637 because these sedimented hydrothermal vents are insufficiently active to host large
638 populations of vent-endemic megafauna, the transfer of chemosynthetic organic matter into
639 the metazoan food web is more limited than in other similar environments. However, through
640 the supply of thermogenic methane to off-axis areas, we demonstrate that hydrothermal
641 circulation can have a much larger spatial extent than previously considered for benthic food
642 webs.

Biogeosciences Discuss., doi:10.5194/bg-2016-318, 2016
Manuscript under review for journal Biogeosciences
Published: 31 August 2016

6. Acknowledgements

JBB was funded by a NERC PhD Studentship (NE/L501542/1). This work was funded by the NERC ChEsSo consortium (Chemosynthetically-driven Ecosystems South of the Polar Front, NERC Grant NE/DOI249X/I). Elemental analyses were funded by the NERC Life Sciences Mass Spectrometry Facility (Proposal no. EK234-13/14). We thank Barry Thornton and the James Hutton Laboratory, Aberdeen for processing the PLFA samples. We also thank Will Goodall-Copestake for assistance in processing the 16S sequence data. We are grateful to the Master and Crew of RRS *James Cook* cruise 055 for technical support and the Cruise Principal Scientific Officer Professor Paul Tyler.

7. Ethics Statement

In accordance with the Antarctic Act (1994) and the Antarctic Regulations (1995), necessary permits (S5-4/2010) were acquired from the South Georgia and South Sandwich Islands Government.

8. Author contributions

Conceived and designed the sampling programme: WDKR, DAP, AGG, CJS & CW. Sample laboratory preparation and isotopic analyses: JBB, JN & CJS. Microbial sequencing: DAP. Statistical analyses: JBB. Produced figures: JBB. Wrote the paper: JBB, CW & WDKR, with contributions and comments from all other authors.

Biogeosciences Discuss., doi:10.5194/bg-2016-318, 2016
Manuscript under review for journal Biogeosciences
Published: 31 August 2016

666 9. References

667

668 Adams TS, Sterner RW (2000) The effect of dietary nitrogen content on trophic level ^{15}N
669 enrichment. Limnology & Oceanography 45:601-607
670 Aquilina A, Connelly DP, Copley JT, Green DR, Hawkes JA, Hepburn L, Huvenne VA, Marsh L,
671 Mills RA, Tyler PA (2013) Geochemical and Visual Indicators of Hydrothermal Fluid
672 Flow through a Sediment-Hosted Volcanic Ridge in the Central Bransfield Basin
673 (Antarctica). Plos One 8:e54686
674 Bell JB, Aquilina A, Woulds C, Glover AG, Little CTS, Reid WDK, Hepburn LE, Newton J, Mills RA
675 (Accepted) Geochemistry, faunal composition and trophic structure at an area of weak
676 methane seepage on the southwest South Georgia margin. Royal Society Open Science
677 Bell JB, Woulds C, Brown LE, Little CTS, Sweeting CJ, Reid WDK, Glover AG (2016) Macrofaunal
678 ecology of sedimented hydrothermal vents in the Bransfield Strait, Antarctica. Frontiers
679 in Marine Science 3:32
680 Bemis K, Lowell R, Farough A (2012) Diffuse Flow On and Around Hydrothermal Vents at Mid-
681 Ocean Ridges. Oceanography 25:182-191
682 Bernardino AF, Levin LA, Thurber AR, Smith CR (2012) Comparative Composition, Diversity
683 and Trophic Ecology of Sediment Macrofauna at Vents, Seeps and Organic Falls. Plos
684 ONE 7:e33515
685 Bernardino AF, Smith CR (2010) Community structure of infaunal macrobenthos around
686 vestimentiferan thickets at the San Clemente cold seep, NE Pacific. Marine Ecology-an
687 Evolutionary Perspective 31:608-621
688 Biomatters (2014) Geneious.
689 Bligh EG (1959) A rapid method of total lipid extration and purification. Canadian Journal of
690 Biochemistry and Phsiology 37:911-917
691 Boetius A, Ravenschlag K, Schubert CJ, Rickert D, Widdel F, Gieseke A, Amman R, Jørgensen BB,
692 Witte U, Pfannkuche O (2000) A marine microbial consortium apparently mediating
693 anaerobic oxidation of methane. Nature 407:623-626
694 Bondoso J, Albuquerque L, Lobo-da-Cunha A, da Costa MS, Harder J, Lage OM (2014)
695 Rhodopirellula lusitana sp. nov. and Rhodopirellula rubra sp. nov., isolated from the
696 surface of macroalgae. Syst Appl Microbiol 37:157-164
697 Boschker HT, Middelburg JJ (2002) Stable isotopes and biomarkers in microbial ecology. FEMS
698 Microbiology Ecology 40:85-95
699 Boschker HT, Vasquez-Cardenas D, Bolhuis H, Moerdijk-Poortvliet TW, Moodley L (2014)
700 Chemoautotrophic carbon fixation rates and active bacterial communities in intertidal
701 marine sediments. PLoS One 9:e101443
702 Canfield DE (2001) Isotope fractionation by natural populations of sulfate-reducing bacteria.
703 Geochimica Et Cosmochimica Acta 65:1117-1124
704 Cerqueira T, Pinho D, Egas C, Froufe H, Altermark B, Candeias C, Santos RS, Bettencourt R
705 (2015) Microbial diversity in deep-sea sediments from the Menez Gwen hydrothermal
706 vent system of the Mid-Atlantic Ridge. Mar Genomics
707 Clarke KR, Somerfield PJ, Gorley RN (2008) Testing of null hypotheses in exploratory
708 community analyses: similarity profiles and biota-environment linkage. Journal of
709 Experimental Marine Biology and Ecology 366:56-69
710 Colaço A, Desbruyères D, Guezennec J (2007) Polar lipid fatty acids as indicators of trophic
711 associations in a deep-sea vent system community. Marine Ecology 28:15-24

712 Connolly RM, Schlacher TA (2013) Sample acidification significantly alters stable isotope ratios
713 of sulfur in aquatic plants and animals. Marine Ecology Progress Series 493:1-8
714 Dekas AE, Chadwick GL, Bowles MW, Joye SB, Orphan VJ (2014) Spatial distribution of nitrogen
715 fixation in methane seep sediment and the role of the ANME archaea. Environ Microbiol
716 16:3012-3029
717 Dekas AE, Poretsky RS, Orphan VJ (2009) Deep-sea archaea fix and share nitrogen in methane-
718 consuming microbial consortia. Science 326:422-426
719 Dhillon A, Teske A, Dillon J, Stahl DA, Sogin ML (2003) Molecular Characterization of Sulfate-
720 Reducing Bacteria in the Guaymas Basin. Applied and environmental microbiology
721 69:2765-2772
722 Dowell F, Cardman Z, Dasarathy S, Kellerman M, Lipp JS, Ruff SE, Biddle JF, McKay L, MacGregor
723 BJ, Lloyd KG, Albert DB, Mendlovitz H, Hinrichs KU, Teske A (2016) Microbial
724 communities in methane- and short chain alkane- rich hydrothermal sediments of
725 Guaymas Basin. Frontiers in microbiology
726 Eichinger I, Hourdez S, Bright M (2013) Morphology, microanatomy and sequence data of
727 *Sclerolinum contortum* (Siboglindae, Annelida) of the Gulf of Mexico. Organisms
728 Diversity & Evolution 13:311-329
729 Eichinger I, Schmitz-Esser S, Schmid M, Fisher CR, Bright M (2014) Symbiont-driven sulfur
730 crystal formation in a thiotrophic symbiosis from deep-sea hydrocarbon seeps. Environ
731 Microbiol Rep 6:364-372
732 Elias-Piera F, Rossi S, Gili JM, Orejas C (2013) Trophic ecology of seven Antarctic gorgonian
733 species. Marine Ecology Progress Series 477:93-106
734 Erickson KL, Macko SA, Van Dover CL (2009) Evidence for a chemotrophically based food web
735 at inactive hydrothermal vents (Manus Basin). Deep Sea Research Part II: Topical
736 Studies in Oceanography 56:1577-1585
737 Frank KL, Rogers DR, Olins HC, Vidoudez C, Girguis PR (2013) Characterizing the distribution
738 and rates of microbial sulfate reduction at Middle Valley hydrothermal vents. ISME J
739 7:1391-1401
740 Gebruk A, Krylova E, Lein A, Vinogradov G, Anderson E, Pimenov N, Cherkashev G, Crane K
741 (2003) Methane seep community of the Håkon Mosby mud volcano (the Norwegian
742 Sea): composition and trophic aspects. Sarsia: North Atlantic Marine Science 88:394-
743 403
744 Georgieva M, Wiklund H, Bell JB, Eilersten MH, Mills RA, Little CTS, Glover AG (2015) A
745 chemosynthetic weed: the tubeworm *Sclerolinum contortum* is a biploar, cosmopolitan
746 species. BMC Evolutionary Biology 15:280
747 Gollner S, Govenar B, Fisher CR, Bright M (2015) Size matters at deep-sea hydrothermal vents:
748 different diversity and habitat fidelity patterns of meio- and macrofauna. Marine
749 Ecology Progress Series 520:57-66
750 Henley SF, Annett AL, Ganeshram RS, Carson DS, Weston K, Crosta X, Tait A, Dougans J, Fallick
751 AE, Clarke A (2012) Factors influencing the stable carbon isotopic composition of
752 suspended and sinking organic matter in the coastal Antarctic sea ice environment.
753 Biogeosciences 9:1137-1157
754 Hothorn T, van de Wiel MA, Zeilis A (2015) Package 'Coin': Conditional Inference Procedures in
755 a Permutation Test Framework. cranr-projectorg
756 Hugler M, Sievert SM (2011) Beyond the Calvin cycle: autotrophic carbon fixation in the ocean.
757 Annual review of marine science 3:261-289
758 Iken K, Brey T, Wand U, Voight J, Junghans P (2001) Trophic relationships in the benthic
759 community at Porcupine Abyssal Plain (NE Atlantic): a stable isotope analysis. Progress
760 in Oceanography 50:383-405

Biogeosciences Discuss., doi:10.5194/bg-2016-318, 2016
Manuscript under review for journal Biogeosciences
Published: 31 August 2016

761 Inskeep WP, Jay ZJ, Macur RE, Clingenpeel S, Tenney A, Lovalvo D, Beam JP, Kozubal MA,
762 Shanks WC, Morgan LA, Kan J, Gorby Y, Yooseph S, Nealson K (2015) Geomicrobiology of
763 sublacustrine thermal vents in Yellowstone Lake: geochemical controls on microbial
764 community structure and function. Frontiers in microbiology 6:1044
765 Jackson AL, Inger R, Parnell AC, Bearhop S (2011) Comparing isotopic niche widths among and
766 within communities: SIBER - Stable Isotope Bayesian Ellipses in R. The Journal of animal
767 ecology 80:595-602
768 Jaeschke A, Eickmann B, Lang SQ, Bernasconi SM, Strauss H, Fruh-Green GL (2014)
769 Biosignatures in chimney structures and sediment from the Loki's Castle low-
770 temperature hydrothermal vent field at the Arctic Mid-Ocean Ridge. Extremophiles
771 18:545-560
772 Kallmeyer J, Boetius A (2004) Effects of Temperature and Pressure on Sulfate Reduction and
773 Anaerobic Oxidation of Methane in Hydrothermal Sediments of Guaymas Basin. Applied
774 and environmental microbiology 70:1231-1233
775 Kharlamenko VI, Zhukova NV, Khotimchenko SV, Svetashev VI, Kamenev GM (1995) Fatty-
776 acids as markers of food sources in a shallow-water hydrothermal ecosystem
777 (Kraternaya Bight, Yankich island, Kurile Islands). Marine Ecology Progress Series
778 120:231-241
779 Klouche N, Basso O, Lascourréges J-F, Cavol J-L, Thomas P, Fauque G, Fardeau M-L, Magot M
780 (2009) Desulfocurvus vexinensis gen. nov., sp. nov., a sulfate-reducing bacterium
781 isolated from a deep subsurface aquifer. International Journal of Systematic and
782 Evolutionary Microbiology 30:3100-3104
783 Larsen K (2006) Tanaidacea (Crustacea; Peracarida) from chemically reduced habitats—the
784 hydrothermal vent system of the Juan de Fuca Ridge, Escabana Trough and Gorda Ridge,
785 northeast Pacific. Zootaxa 1164:1-33
786 Layman CA, Arrington DA, Montaña CG, Post DM (2007) Can Stable Isotope Ratios Provide For
787 Community-Wide Measures of Trophic Structure? Ecology 88:42-48
788 Levin LA, Baco AR, Bowden D, Colaço A, Cordes E, Cunha MR, Demopoulos A, Gobin J, Grupe B,
789 Le J, Metaxas A, Netburn A, Rouse GW, Thurber AR, Tunnicliffe V, Van Dover C,
790 Vanreusel A, Watling L (2016) Hydrothermal Vents and Methane Seeps: Rethinking the
791 Sphere of Influence. Frontiers in Marine Science 3:72
792 Levin LA, Mendoza GF, Konotchick T, Lee R (2009) Macrobenthos community structure and
793 trophic relationships within active and inactive Pacific hydrothermal sediments. Deep
794 Sea Research Part II: Topical Studies in Oceanography 56:1632-1648
795 Levin LA, Orphan VJ, Rouse GW, Rathburn AE, Ussler W, III, Cook GS, Goffredi SK, Perez EM,
796 Waren A, Grupe BM, Chadwick G, Strickrott B (2012) A hydrothermal seep on the Costa
797 Rica margin: middle ground in a continuum of reducing ecosystems. Proceedings of the
798 Royal Society B-Biological Sciences 279:2580-2588
799 Levin LA, Ziebis W, Mendoza GF, Bertics VJ, Washington T, Gonzalez J, Thurber AR, Ebbed B,
800 Lee RW (2013) Ecological release and niche partitioning under stress: Lessons from
801 dorvilleid polychaetes in sulfidic sediments at methane seeps. Deep-Sea Research Part
802 II-Topical Studies in Oceanography 92:214-233
803 Main CE, Ruhl HA, Jones DOB, Yool A, Thornton B, Mayor DJ (2015) Hydrocarbon
804 contamination affects deep-sea benthic oxygen uptake and microbial community
805 composition. Deep Sea Research Part I: Oceanographic Research Papers 100:79-87
806 Martens CS (1990) Generation of short chain organic acid anions in hydrothermally altered
807 sediments of the Guaymas Basin, Gulf of California. Applied Geochemistry 5:71-76
808 McClain CR, Schlacher TA (2015) On some hypotheses of diversity of animal life at great depths
809 on the sea floor. Marine Ecology:12288

McKay L, Klokman VW, Mendlovitz HP, LaRowe DE, Hoer DR, Albert D, Amend JP, Teske A (2015) Thermal and geochemical influences on microbial biogeography in the hydrothermal sediments of Guaymas Basin, Gulf of California. Environmental Microbiology Reports:n/a-n/a

Ondov BD, Bergman NH, Phillippy AM (2011) Interactive metagenomic visualization in a Web browser. BMC Bioinformatics 30:385

Parnell AC, Inger R, Bearhop S, Jackson AL (2010) Source partitioning using stable isotopes: coping with too much variation. PLoS One 5:e9672

Petersen S, Herzig PM, Schwarz-Schampera U, Hannington MD, Jonasson IR (2004) Hydrothermal precipitates associated with bimodal volcanism in the Central Bransfield Strait, Antarctica. Mineralium Deposita 39:358-379

Phillips DL, Inger R, Bearhop S, Jackson AL, Moore JW, Parnell AC, Semmens BX, Ward EJ (2014) Best practices for use of stable isotope mixing models in food-web studies. Canadian Journal of Zoology 92:823-835

R Core Team (2013) R: A Language and environment for statistical computing. R Foundation for Statistical Computing, Vienna, Austria http://www.R-project.org/.

Rau GH (1981) Low $^{15}N/^{14}N$ in hydrothermal vent animals: ecological implications. Nature 289:484-485

Reid WDK, Sweeting CJ, Wigham BD, McGill RAR, Polunin NVC (2016) Isotopic niche variability in macroconsumers of the East Scotia Ridge (Southern Ocean) hydrothermal vents: what more can we learn from an ellipse? Marine Ecology Progress Series:13-24

Reid WDK, Sweeting CJ, Wigham BD, Zwirglmaier K, Hawkes JA, McGill RAR, Linse K, Polunin NVC (2013) Spatial Differences in East Scotia Ridge Hydrothermal Vent Food Webs: Influences of Chemistry, Microbiology and Predation on Trophodynamics. Plos One 8

Reid WDK, Wigham BD, McGill RAR, Polunin NVC (2012) Elucidating trophic pathways in benthic deep-sea assemblages of the Mid-Atlantic Ridge north and south of the Charlie-Gibbs Fracture Zone. Marine Ecology Progress Series 463:89-103

Rodrigues CF, Hilário A, Cunha MR (2013) Chemosymbiotic species from the Gulf of Cadiz (NE Atlantic): distribution, life styles and nutritional patterns. Biogeosciences 10:2569-2581

Sahling H, Wallman K, Dählmann A, Schmaljohann R, Petersen S (2005) The physicochemical habitat of *Sclerolinum sp.* at Hook Ridge hydrothermal vent, Bransfield Strait, Antarctica. Limnology & Oceanography 50:598-606

Schlesner H (2015) Blastopirellula. Bergey's Manual of Systematics of Archaea and Bacteria. John Wiley & Sons, Ltd

Schmaljohann R, Faber E, Whiticar MJ, Dando PR (1990) Co-existence of methane- and sulphur-based endosymbioses between bacteria and invertebrates at a site in the Skagerrak. Marine Ecology Progress Series 61:11-124

Schmaljohann R, Flügel HJ (1987) Methane-oxidizing bacteria in Pogonophora. Sarsia 72:91-98

Sellanes J, Zapata-Hernández G, Pantoja S, Jessen GL (2011) Chemosynthetic trophic support for the benthic community at an intertidal cold seep site at Mocha Island off central Chile. Estuarine, Coastal and Shelf Science 95:431-439

Soto LA (2009) Stable carbon and nitrogen isotopic signatures of fauna associated with the deep-sea hydrothermal vent system of Guaymas Basin, Gulf of California. Deep Sea Research Part II: Topical Studies in Oceanography 56:1675-1682

Southward A, J., Southward EC, Brattegard T, Bakke T (1979) Further Experiments on the value of Dissolved Organic Matter as Food for *Siboglinum fjiordicum* (Pogonophora). Journal of Marine Biological Asociation of the United Kingdom 59:133-148

Southward EC, Gebruk A, Kennedy H, Southward AJ, Chevaldonne P (2001) Different energy sources for three symbiont-dependent bivalve molluscs at the Logatchev hydrothermal

site (Mid-Atlantic Ridge). Journal of Marine Biological Asociation of the United Kingdom 81:655-661

Sweetman AK, Levin LA, Rapp HT, Schander C (2013) Faunal trophic structure at hydrothermal vents on the southern Mohn's Ridge, Arctic Ocean. Marine Ecology Progress Series 473:115

Tarasov VG, Gebruk AV, Mironov AN, Moskalev LI (2005) Deep-sea and shallow-water hydrothermal vent communities: Two different phenomena? Chemical Geology 224:5-39

Teske A, Callaghan AV, LaRowe DE (2014) Biosphere frontiers of subsurface life in the sedimented hydrothermal system of Guaymas Basin. Frontiers in microbiology 5:362

Teske A, Hinrichs KU, Edgcomb V, de Vera Gomez A, Kysela D, Sylva SP, Sogin ML, Jannasch HW (2002) Microbial Diversity of Hydrothermal Sediments in the Guaymas Basin: Evidence for Anaerobic Methanotrophic Communities. Applied and environmental microbiology 68:1994-2007

Thornhill DJ, Wiley AA, Campbell AL, Bartol FF, Teske A, Halanych KM (2008) Endosymbionts of *Siboglinum fjordicum* and the Phylogeny of Bacterial Endosymbionts in Siboglinidae (Annelida). Biological Bulletin 214:135-144

Thornton B, Zhang Z, Mayes RW, Högberg MN, Midwood AJ (2011) Can gas chromatography combustion isotope ratio mass spectrometry be used to quantify organic compound abundance? Rapid Communications in Mass Spectrometry 25:2433-2438

Tyler PA, Connelly DP, Copley JT, Linse K, Mills RA, Pearce DA, Aquilina A, Cole C, Glover AG, Green DR, Hawkes JA, Hepburn L, Herrera S, Marsh L, Reid WD, Roterman CN, Sweeting CJ, Tate A, Woulds C, Zwirglmaier K (2011) RRS *James Cook* cruise JC55: Chemosynthetic Ecosystems of the Southern Ocean. BODC Cruise Report

Valls M, Olivar MP, Fernández de Puelles ML, Molí B, Bernal A, Sweeting CJ (2014) Trophic structure of mesopelagic fishes in the western Mediterranean based on stable isotopes of carbon and nitrogen. Journal of Marine Systems 138:160-170

Vetter RD, Fry B (1998) Sulfur contents and sulfur-isotope compositions of thiotrophic symbioses in bivalve molluscs and vestimentiferan worms. Marine Biology 132:453-460

Walker BD, McCarthy MD, Fisher AT, Guilderson TP (2008) Dissolved inorganic carbon isotopic composition of low-temperature axial and ridge-flank hydrothermal fluids of the Juan de Fuca Ridge. Marine Chemistry 108:123-136

Wang Q, Garrity GM, Tiedje JM, Cole JR (2007) Naïve Bayesian Classifier for Rapid Asssignment of rRNA sequences into the New Bacterial Taxonomy. Applied Environmental Microbiology 73:5261-5267

Weber A, Jørgensen BB (2002) Bacterial sulfate reduction in hydrothermal sediments of the Guaymas Basin, Gulf of California, Mexico. Deep-Sea Research I 49:827-841

Whitaker D, Christmann M (2013) Package 'clustsig'. cranr-projectorg

Whiticar MJ (1999) Carbon and Hydrogen isotope systematics of bacterial formation and oxidation of methane. Chemical Geology 161:291-314

Whiticar MJ, Suess E (1990) Hydrothermal hydrocarbon gases in the sediments of the King George Basin, Bransfield Strait, Antarctica. Applied Geochemistry 5:135-147

Woolley SNC, Tittensor DP, Dunstan PK, Guillera-Arroita G, Lahoz-Monfort JJ, Wintle BA, Worm B, O'Hara TD (2016) Deep-sea diversity patterns are shaped by energy availability. Nature

Wu Y, Cao Y, Wang C, Wu M, Aharon O, Xu X (2014) Microbial community structure and nitrogenase gene diversity of sediment from a deep-sea hydrothermal vent field on the Southwest Indian Ridge. Acta Oceanologica Sinica 33:94-104

Biogeosciences Discuss., doi:10.5194/bg-2016-318, 2016
Manuscript under review for journal Biogeosciences
Published: 31 August 2016

907 Yorisue T, Inoue K, Miyake H, Kojima S (2012) Trophic structure of hydrothermal vent
908 communities at Myojin Knoll and Nikko Seamount in the northwestern Pacific:
909 Implications for photosynthesis-derived food supply. Plankton and Benthos Research
910 7:35-40
911 Yoshinaga MY, Holler T, Goldhammer T, Wegener G, Pohlman JW, Brunner B, Kuypers MMM,
912 Hinrichs K-U, Elvert M (2014) Carbon isotope equilibration during sulphate-limited
913 anaerobic oxidation of methane. Nature Geoscience
914 Young JN, Bruggeman J, Rickaby REM, Erez J, Conte M (2013) Evidence for changes in carbon
915 isotopic fractionation by phytoplankton between 1960 and 2010. Global
916 Biogeochemical Cycles 27:505-515
917

918

Biogeosciences Discuss., doi:10.5194/bg-2016-318, 2016
Manuscript under review for journal Biogeosciences
Published: 31 August 2016

919 10. Figure captions

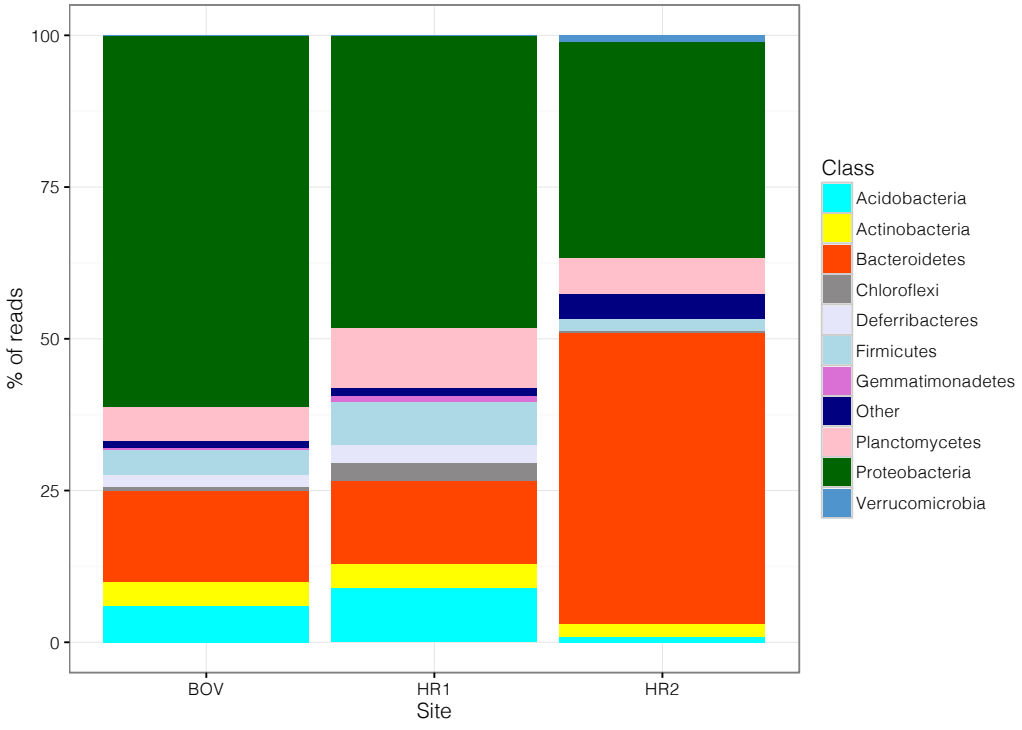

920

921 Fig. 1 – Microbial composition (classes) at the off-vent/ off-axis site (BOV) and the two Hook
922 Ridge sites (HR1 and HR2). Archaea excluded from figure as they only accounted for 0.008 %
923 of reads at HR2 and were not found elsewhere.

Biogeosciences Discuss., doi:10.5194/bg-2016-318, 2016
Manuscript under review for journal Biogeosciences
Published: 31 August 2016

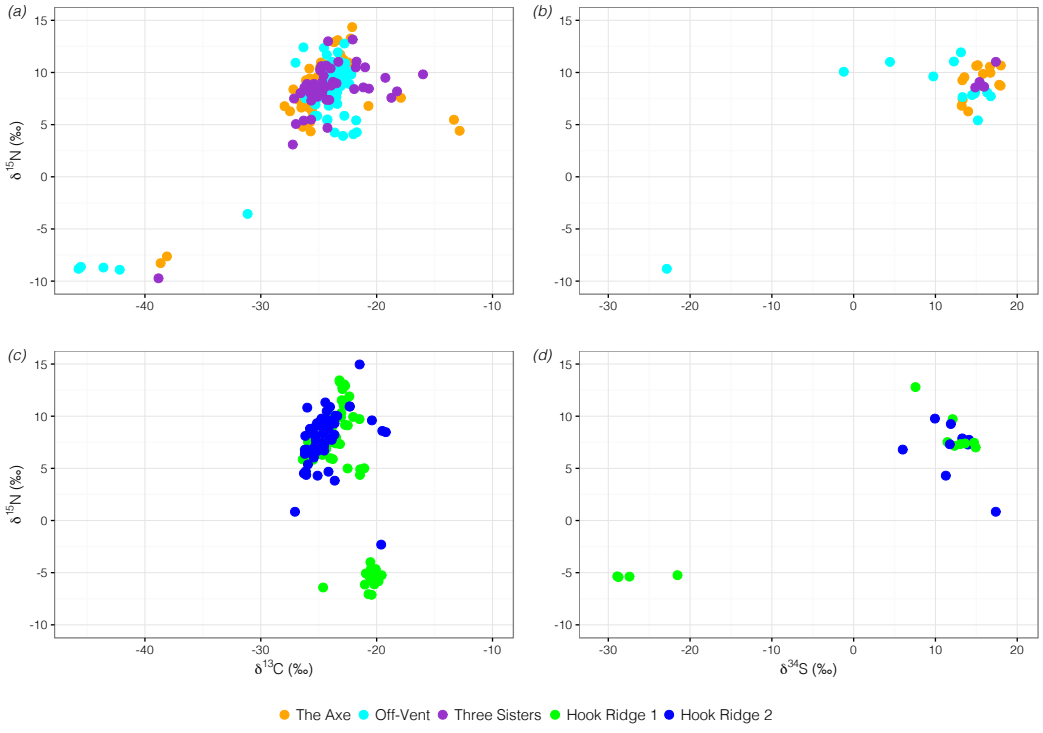

924

925 Fig. 2 – Carbon-Nitrogen and Sulphur-Nitrogen biplots for bulk isotopic signatures of benthos,

926 separated into non-vent (top) and vent sites (bottom).

Biogeosciences Discuss., doi:10.5194/bg-2016-318, 2016
Manuscript under review for journal Biogeosciences
Published: 31 August 2016

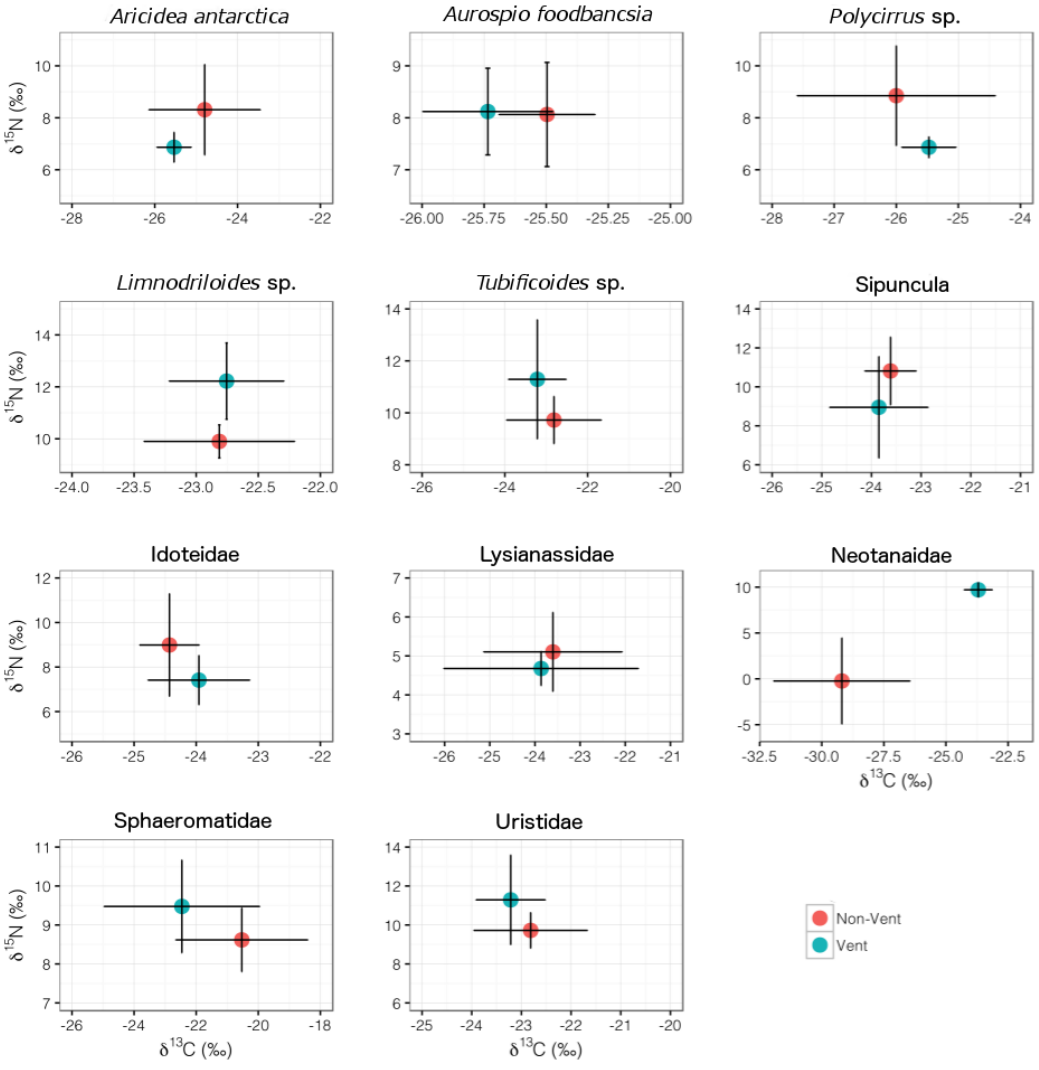

Fig. 3 – Biplot of CN isotopic data from species sampled both at vents and non-vent background regions. Mean ± standard deviation, X-Y scales vary

Biogeosciences Discuss., doi:10.5194/bg-2016-318, 2016
Manuscript under review for journal Biogeosciences
Published: 31 August 2016

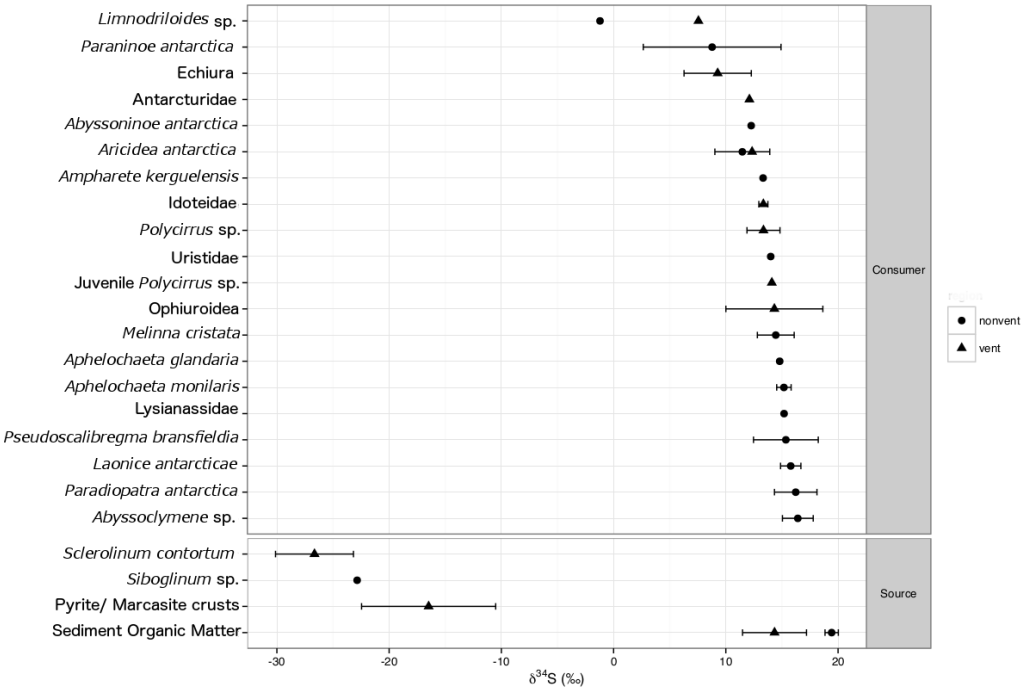

931

932 Fig. 4 – Plot of $\delta^{34}S$ measurements by discriminated by species and habitat (vent/ non-vent).

933 Data for $\delta^{34}S$ in crusts from Petersen et al. (2004)

Biogeosciences Discuss., doi:10.5194/bg-2016-318, 2016
Manuscript under review for journal Biogeosciences
Published: 31 August 2016

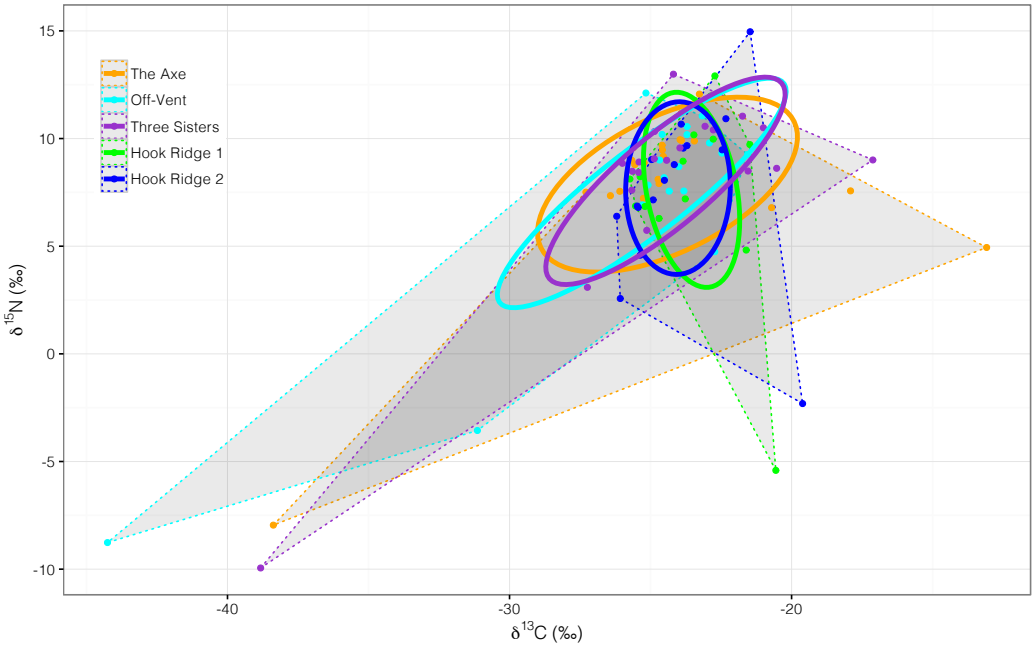

934

935 Fig 5 – Faunal isotopic signatures (mean per species), grouped by site with total area (shaded

936 area marked by dotted lines) and sample-size corrected standard elliptical area (solid lines)

937

938

Biogeosciences Discuss., doi:10.5194/bg-2016-318, 2016
Manuscript under review for journal Biogeosciences
Published: 31 August 2016

939 11. Tables

Isotope	Species	Idoteidae	*Polycirrus* sp.	*Aphelochaeta glandaria*	Phyllodocida sp.
	Treatment	0.1M HCl	0.1M HCl	0.1M HCl	1.0M HCl
$\delta^{13}C$	Difference in mean	1.59	0.18	0.41	0.90
(‰)	σ untreated	0.72	0.30	0.2	0.50
	σ treated	0.67	0.33	0.23	0.16
	Population range	2.86	3.04	2.72	-
$\delta^{15}N$	Difference in mean	0.92	0.17	0.10	0.88
(‰)	σ untreated	0.22	0.30	0.19	0.35
	σ treated	1.00	0.18	0.15	0.34
	Population range	3.42	4.57	5.75	-
$\delta^{34}S$	Difference in mean	-	-	0.36	1.13
(‰)	σ untreated	-	-	0.44	0.82
	σ treated	-	-	0.68	1.39
	Population range	-	-	2.32	-

940

941 Table 1 – Differences in isotopic values and standard deviation (σ) of ethanol preserved fauna
942 sampled during JC55 in response to acid treatment, compared with population ranges of
943 untreated samples. Phyllodocida sp. was a single large specimen, used only as part of
944 preliminary experiments.

945

Biogeosciences Discuss., doi:10.5194/bg-2016-318, 2016
Manuscript under review for journal Biogeosciences
Published: 31 August 2016

946

	Bransfield Off-Vent			Three Sisters		
PLFA	nM g^{-1}	%	$\delta^{13}C$ (‰)	nM g^{-1}	%	$\delta^{13}C$ (‰)
i14:0	0.03	0.12	-22.07	0.02	0.09	-27.96
14:0	0.80	3.04	-31.21	0.83	3.43	-30.90
i15:0	0.76	2.89	-28.57	0.76	3.13	-28.05
a15:0	1.06	4.03	-28.35	1.06	4.39	-27.71
15:0	0.30	1.13	-29.30	0.19	0.77	-29.82
i16:1	0.11	0.44	-31.40	0.02	0.10	-20.31
16:1w11c	0.00	0.00	n.d.	0.06	0.24	-23.13
i16:0	0.34	1.30	-28.51	0.30	1.24	-27.81
16:1w11t	0.78	2.98	-24.42	0.66	2.75	-25.03
16:1w7c	3.98	15.19	-28.92	3.37	13.95	-28.13
16:1w5c	1.12	4.27	-34.05	0.96	3.99	-34.02
16:0	4.29	16.37	-31.10	3.80	15.73	-29.99
br17:0	0.00	0.00	n.d.	0.00	0.00	n.d.
10-Me-16:0	0.46	1.77	-28.52	0.45	1.87	-29.09
i17:0	0.08	0.32	-33.20	0.20	0.84	-29.79
a17:0	0.25	0.97	-31.94	0.21	0.87	-31.29
12-Me-16:0	0.25	0.94	-32.92	0.21	0.86	-31.59
17:1w8c	0.13	0.50	-34.08	0.11	0.44	-31.27
17:0cy	0.33	1.26	-36.20	0.27	1.10	-32.83
17:0	0.15	0.56	-39.96	0.08	0.33	-50.39
10-Me-17:0	0.00	0.00	n.d.	0.00	0.00	n.d.
18:3w6,8,13	0.67	2.55	-34.64	0.69	2.87	-33.83
18:2w6,9	0.12	0.46	-27.81	0.09	0.36	-52.17
18:1w9	1.13	4.30	-29.96	1.33	5.50	-29.90
18:1w7	4.42	16.85	-29.01	3.84	15.91	-29.07
18:1w(10 or 11)	2.33	8.88	-30.12	2.26	9.36	-29.93
18:0	0.66	2.50	-30.60	0.54	2.22	-30.62
19:1w6	0.03	0.12	-23.45	0.03	0.12	-30.05
10-Me-18:0	0.00	0.00	n.d.	0.00	0.00	n.d.
19:1w8	0.11	0.42	-56.57	0.17	0.69	-37.46
19:0cy	0.20	0.77	-35.55	0.20	0.83	-34.80
20:4(n-6)	0.14	0.55	-39.95	0.20	0.83	-34.07
20:5(n-3)	0.41	1.57	-37.99	0.30	1.23	-39.28
20:1(n-9)	0.42	1.60	-31.54	0.41	1.71	-33.73
22:6(n-3)	0.22	0.83	-34.13	0.43	1.77	-29.95
22:1(n-9)	0.10	0.39	-31.29	0.10	0.41	-29.86
24:1(n-9)	0.03	0.12	-28.70	0.02	0.07	-29.65
Total	26.23			24.15		
Average	0.71		-30.53	0.65		-30.11

Biogeosciences Discuss., doi:10.5194/bg-2016-318, 2016
Manuscript under review for journal Biogeosciences
Published: 31 August 2016

	mg C m^{-2}	$\delta^{13}C$ (‰)	mg C m^{-2}	$\delta^{13}C$ (‰)
Bacterial Biomass	134.50	-26.83	197.12	-26.41

947

948

	Hook Ridge 1		Hook Ridge 2			Range $\delta^{13}C$
PLFA	nM g^{-1}	$\delta^{13}C$ (‰)	nM g^{-1}	%	$\delta^{13}C$ (‰)	(‰)
i14:0	0.03	-15.67	0.10	0.80	-28.79	-13.12
14:0	0.80	-32.70	0.80	6.40	-29.56	-3.13
i15:0	0.76	-29.72	0.40	3.20	-28.11	-1.67
a15:0	1.06	-29.10	0.90	7.20	-28.94	-1.40
15:0	0.30	-29.01	0.30	2.40	-28.33	-1.49
i16:1	0.11	-27.57	0.00	0.00	n.d.	-11.09
16:1w11c	0.00	-17.44	0.00	0.00	n.d.	-5.70
i16:0	0.34	-29.43	0.20	1.60	-28.79	-1.62
16:1w11t	0.78	-25.79	0.30	2.40	-8.65	-17.15
16:1w7c	3.98	-29.21	2.50	20.00	-22.92	-6.30
16:1w5c	1.12	-31.17	0.30	2.40	-24.33	-9.72
16:0	4.29	-31.83	3.30	26.40	-29.33	-2.50
br17:0	0.00	-22.92	0.00	0.00	-15.76	-7.17
10-Me-16:0	0.46	-30.28	0.20	1.60	-41.29	-12.77
i17:0	0.08	n.d.	0.00	0.00	n.d.	-3.41
a17:0	0.25	-29.02	0.20	1.60	-28.58	-3.37
12-Me-16:0	0.25	-28.60	0.10	0.80	-28.23	-4.69
17:1w8c	0.13	-27.14	0.10	0.80	-27.23	-6.94
17:0cy	0.33	-32.30	0.20	1.60	-27.66	-8.54
17:0	0.15	-40.03	0.20	1.60	-30.81	-19.58
10-Me-17:0	0.00	-34.98	0.00	0.00	n.d.	0.00
18:3w6,8,13	0.67	-31.16	0.50	4.00	-29.04	-5.60
18:2w6,9	0.12	-29.96	0.30	2.40	-26.65	-25.52
18:1w9	1.13	-29.64	0.40	3.20	-25.58	-4.38
18:1w7	4.42	-29.87	0.60	4.80	-24.74	-5.12
18:1w(10 or 11)	2.33	-31.89	0.00	1.60	n.d.	-1.96
18:0	0.66	-29.42	0.30	0.00	-29.86	-1.20
19:1w6	0.03	-26.21	0.00	2.40	n.d.	-6.60
10-Me-18:0	0.00	-25.36	0.00	0.00	n.d.	0.00
19:1w8	0.11	-41.19	0.00	0.00	n.d.	-19.11

Biogeosciences Discuss., doi:10.5194/bg-2016-318, 2016
Manuscript under review for journal Biogeosciences
Published: 31 August 2016

19:0cy	0.20	-30.47	0.10	0.00	-28.70	-6.85
20:4(n-6)	0.14	n.d.	0.00	0.80	n.d.	-5.89
20:5(n-3)	0.41	n.d.	0.00	0.00	n.d.	-1.29
20:1(n-9)	0.42	n.d.	0.00	0.00	n.d.	-2.18
22:6(n-3)	0.22	n.d.	0.00	0.00	n.d.	-4.18
22:1(n-9)	0.10	n.d.	0.00	0.00	n.d.	-1.43
24:1(n-9)	0.03	n.d.	0.00	0.00	n.d.	-0.95
Total	26.23		12.30			
Average	0.71	-30.25	0.33		-26.87	

Bacterial Biomass	**$\delta^{13}C$ (‰)**	**mg C m^{-2}**	**$\delta^{13}C$ (‰)**
	-26.55	85.45	-23.17

Table 2 – PLFA profiles from freeze-dried sediment (nM per g dry sediment). PLFA names relate to standard notation (i = iso; a = anti-iso; first number = number of carbon atoms in chain; ω = double bond; Me = methyl group). N.P. = Not present in sample. Total PLFA $\delta^{13}C$ measurements weighted by concentration Bulk bacterial $\delta^{13}C$ estimated from average conversion factor ($\delta^{13}C$ in PLFA depleted compared to bulk bacterial biomass by 3.7 ‰ (Boschker & Middelburg 2002)). No data = n.d. N. B. Table split to conform to submission portal requirements.

Biogeosciences Discuss., doi:10.5194/bg-2016-318, 2016
Manuscript under review for journal Biogeosciences
Published: 31 August 2016

958

Isotope	Vents ‰ (± S.D.)	Non-Vent ‰ (± S.D.)	Different? (T-Test, df = 3)
$\delta^{13}C$	-26.22 (± 0.41)	-25.80 (± 0.26)	No
$\delta^{15}N$	5.73 (± 0.71)	5.00 (± 0.30)	No
$\delta^{34}S$	14.34 (± 2.85)	19.43 (± 0.59)	Yes ($T = 3.49$, $p < 0.05$)

959

960 Table 3 – Mean isotopic signatures of sediment organic matter.

Biogeosciences Discuss., doi:10.5194/bg-2016-318, 2016
Manuscript under review for journal Biogeosciences
Published: 31 August 2016

961

Site	Ellipse							Nearest Neighbour Distance	
	SEAc (‰²)	SEA.B (‰²)	Cred. (95% ± ‰²)	TA (‰²)	Θ	E	CD	Mean	S.D.
The Axe	49.27	45.00	19.93	161.64	0.67	0.85	3.59	1.76	4.17
Off-Vent	39.81	36.52	16.82	139.12	0.81	0.97	4.34	2.13	3.88
Three Sisters	35.46	32.61	14.71	110.24	0.86	0.95	3.85	1.93	3.78
Hook Ridge 1	23.10	20.66	11.17	42.59	-1.43	0.94	3.30	1.64	2.60
Hook Ridge 2	23.38	21.08	10.73	61.79	1.55	0.89	3.17	1.52	2.03
Mean									
Non-Vent	**41.51**	**38.04**	**17.15**	**137.00**	**0.78**	**0.92**	**3.93**	**1.94**	**3.94**
Vent	**23.24**	**20.87**	**10.95**	**52.19**	**0.10**	**0.91**	**3.23**	**1.58**	**2.31**

962

Site	Centroid				
	$\delta^{13}C$ (‰)	$\delta^{15}N$ (‰)	$\delta^{34}S$ (‰)	dNr (‰)	dCr (‰)
The Axe	-24.39	7.86		20.02	25.29
Off-Vent	-25.31	7.47	8.07	20.88	22.70
Three Sisters	-24.47	8.04		22.94	21.71
Hook Ridge 1	-23.54	7.62	5.42	18.32	5.18
Hook Ridge 2	-24.02	7.70		17.27	6.59

Biogeosciences Discuss., doi:10.5194/bg-2016-318, 2016
Manuscript under review for journal Biogeosciences
Published: 31 August 2016

Mean				
Non-Vent	**-24.72**	**7.79**	**21.28**	**23.23**
Vent	**-23.78**	**7.66**	**17.80**	**5.88**

963

964 Table. 4 – Ellipse Area & Layman Metrics of benthos by site. SEAc = Sample-sized corrected
965 standard elliptical area; SEA.B = Bayesian estimate of standard elliptical area; TA = Total hull
966 area; E = Eccentricity; dNr = Nitrogen range; dCr = Carbon range; dSr = Sulphur range; CD =
967 Centroid distance. Note: dSR reported only for Hook Ridge 1 and the off-vent site since $\delta^{34}S$
968 values of siboglinids were only measured from these sites; hence dSr at other sites would be a
969 considerable underestimate. As $\delta^{34}S$ values were comparatively under-representative, these
970 values were not used in calculation of any other metric. N. B. Table split to conform to
971 submission portal requirements.